Beyond the fringe: Ultrafast pulse measurement using interferometry

Ian A. Walmsley

Department of Physics
Clarendon Laboratory
University of Oxford

Outline

I . Introduction
II.General principles of pulse characterization
III. SPIDER
IV. Spatial coding
V. Long crystals
VI. Into the attosecond regime

Victor Wong, Chris Iaconis, Ellen Kosik,
Aleksandr Radunsky, Adam Wyatt, Dane Austin

Matt Anderson, Christophe Dorrer,
Simon-Pierre Gorza, Piotr Wasylczyk

Introduction

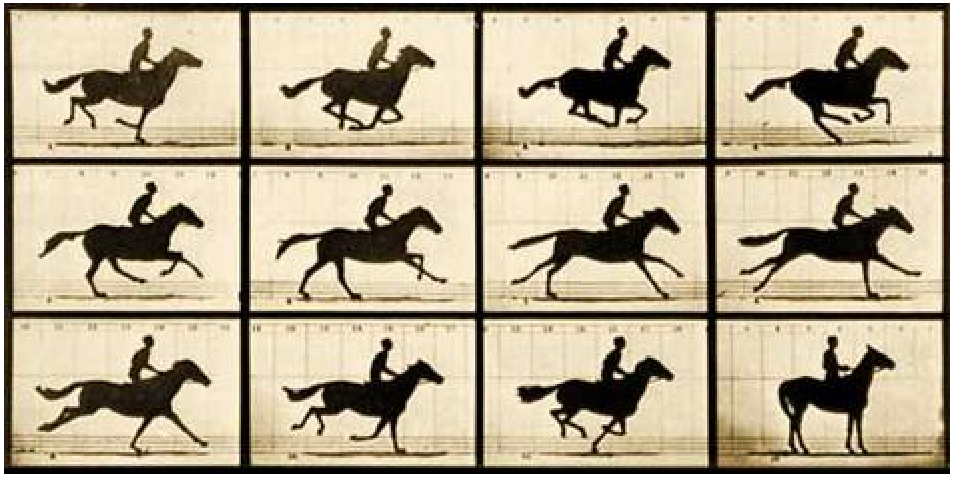

Brief events are probed by briefer ones

(Basic research and wealth creation!)

Briefest propagating electromagnetic pulse is a single cycle.

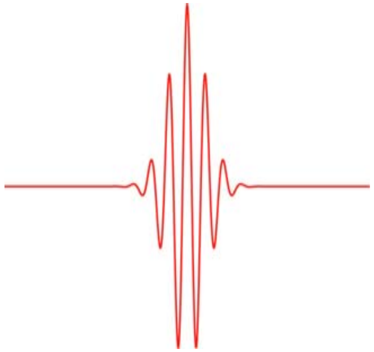

One cycle at 800 nm is approx 2 fs long -
one cycle at 24 nm (30H) is less than 100 as long.

It's out in the field

The electric field is a fundamental entity in Maxwell's theory;

thus it contains the most information one can infer from optical experiments.

Knowledge of the field provides a source performance diagnostic and experimental tool.

$$\tilde{E}(\omega) = \int_{-\infty}^{+\infty} E(t) \exp(-i\omega t) dt = \sqrt{I(\omega)} \exp(i\varphi(\omega))$$

$$E(t) = \frac{1}{2\pi} \int_{-\infty}^{+\infty} \tilde{E}(\omega) \exp(i\omega t) d\omega = \sqrt{I(t)} \exp(i\varphi(t))$$

$I(\omega)$	Spectral density	Measured with a spectrometer
$\varphi(\omega)$	Spectral phase (group delay)	Measurement requires a 'fast' element
$I(t)$	Temporal intensity	
$\varphi(t)$	Temporal phase (instantaneous frequency)	

Long-standing problem in laser science and technology

PROCEEDINGS OF THE IEEE, VOL. 62, NO. 3, MARCH 1974

Ultrashort Pulse Measurements

D. J. BRADLEY AND GEOFFREY H. C. NEW

Invited Paper

Abstract—The generation of intense ultrashort light pulses in mode-locked laser systems has made possible a wide range of new experiments designed to study the interaction of light with matter. For the quantitative interpretation of the results, accurate measurement of the optical pulse structure is essential, and it is the purpose of this paper to review all the diagnostic techniques currently available. The recent rapid development of the electron-optical streak camera is highlighted, while considerable space is devoted to an extensive description of the many second- and higher order correlation measurements (including the popular two-photon fluorescence method). A discussion of ultrafast shutter techniques is also included, together with a section on pulse chirping and dynamic spectroscopy.

I. Introduction

Developments in basic physics are almost always related to advances in measurement techniques. Sometimes new methods of measurement open up new branches of knowledge and at other times new measurement techniques follow. The recent developments in time measurements in the picosecond range have been made possible by the availability of intense ultrashort pulses of light from mode-locked lasers. However, it is to be expected that these very great advances in optical chronography will, in turn, lead to a better understanding of fundamental processes in atomic and molecular physics. Thus it is now possible to investigate on a

its center a small volume of highly compressed high-temperature plasma, with an inertial confinement time of $\sim 10^{-11}$ s [30], [31]. This offers the possibility of controlled thermonuclear fusion. Picosecond measurements are needed for shaping and monitoring the laser pulses to be employed in such plasma compression studies.

For the quantitative interpretation of the results of these and similar experiments, and for the construction of practical devices exploiting ultrashort pulse techniques, accurate measurement of the exciting pulse durations is essential. It is the purpose of this paper to review all the measurement techniques currently available. It would not be appropriate to indulge here in a detailed analysis of the pulse generation processes themselves, neither does space permit it. However, some discussion of this aspect is unavoidable since most of the pulse measurement techniques have been developed originally to study the mechanism of laser mode-locking.

II. The Structure of Ultrashort Pulses

In this section, we consider first the mathematical description of optical pulses and define the terms involved to form a basis for the discussion of the experimental results reviewed in later sections.

Outline

I . Introduction
II.General principles of pulse characterization
III. SPIDER
IV. Spatial coding
V. Long crystals
VI. Into the attosecond regime

*IAW and V. Wong, JOSAB **12,** 491 (1995) ibid **13,** 2453 (1996)*

Linear stationary filters

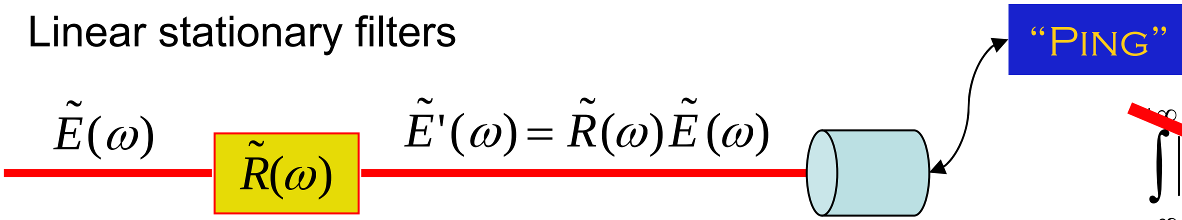

$$\int_{-\infty}^{+\infty} \left|E'(t)\right|^2 dt = \int_{-\infty}^{+\infty} \left|\tilde{E}'(\omega)\right|^2 \frac{d\omega}{2\pi} = \int_{-\infty}^{+\infty} \left|\tilde{R}(\omega)\right|^2 \left|\tilde{E}(\omega)\right|^2 \frac{d\omega}{2\pi}$$

Linear non-stationary filters

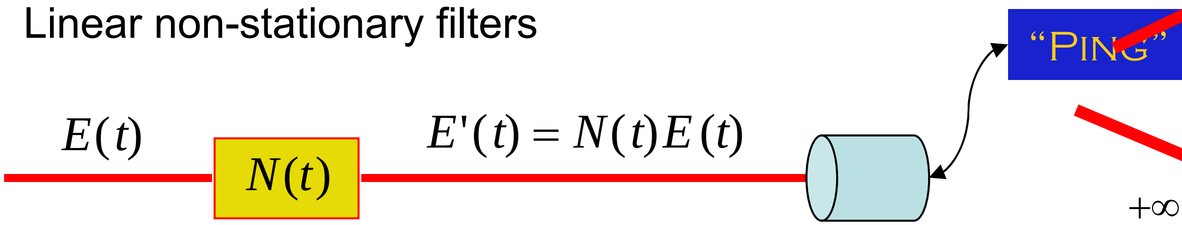

$$\int_{-\infty}^{+\infty} \left|E'(t)\right|^2 dt = \int_{-\infty}^{+\infty} \left|N(t)\right|^2 \left|E(t)\right|^2 dt$$

Phase-sensitivity with integrating detectors requires both stationary and non-stationary filters

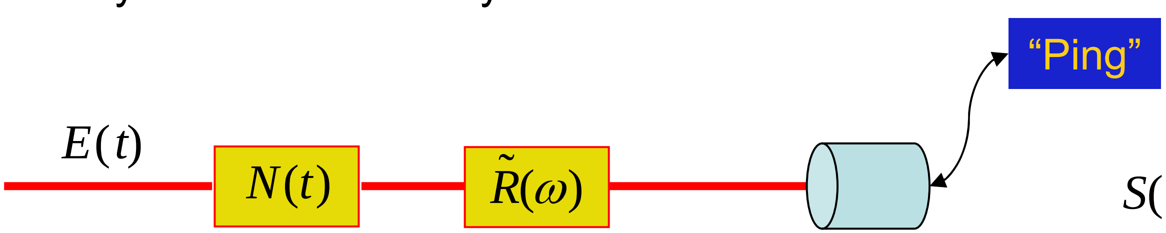

$$S(\{\theta\}) = \Im\left(E(t); \{\theta\}\right)$$

Linear filters

IAW and V. Wong, JOSAB ***12,*** *491 (1995) ibid* ***13,*** *2453 (1996)*

Linear stationary filters

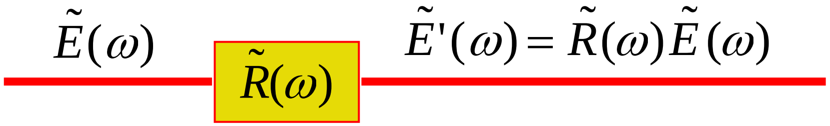

Linear non-stationary filters

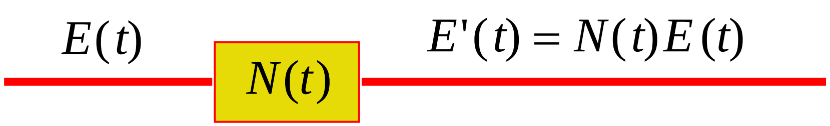

General input-output relation

$$E_{out}(t) = \int dt' \; H(t,t') E_{in}(t')$$

General transfer function:

$$H(t,t') = \frac{1}{\sqrt{2\pi \mathrm{B}}} \exp\left\{ -\frac{i}{2\mathrm{B}} \left(\mathrm{A} t^2 - 2tt' + \Delta t'^2 \right) \right\}$$

Spectrometer

$$\tilde{S}(\omega;\omega_C) = \exp\left[-(\omega - \omega_C)^2 / (2\gamma^2) \right]$$

Dispersive line

$$\tilde{S}_q(\omega;\phi''_\omega) = \exp\left(i\phi''_\omega \omega^2 / 2 \right)$$

Shutter/ time gate

$$N^A(t;\tau) = \exp\left[-\Gamma^2 (t-\tau)^2 / 2 \right]$$

Phase modulator

$$N_q^P(t;\phi''_t) = \exp\left(i\phi''_t t^2 / 2 \right)$$

Transfer matrix:

$$\underline{\underline{T}} = \begin{pmatrix} \mathrm{A} & \mathrm{B} \\ \mathrm{X} & \Delta \end{pmatrix}$$

A classic: the intensity autocorrelator

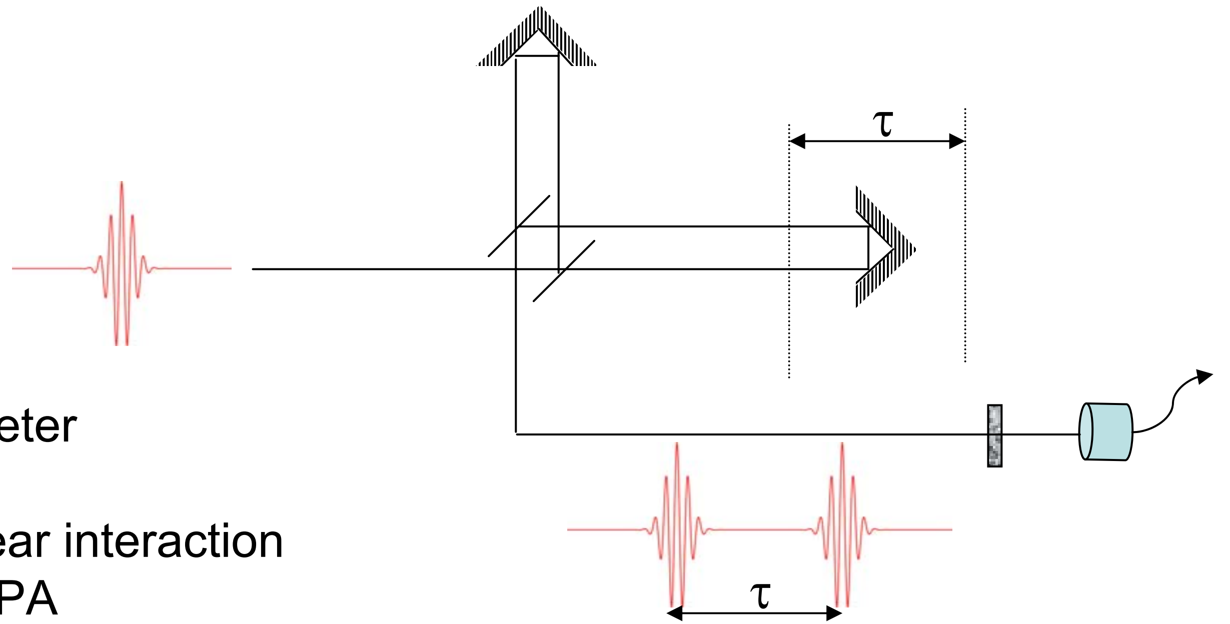

Michelson interferometer

Second-order nonlinear interaction
e.g. SHG, TPA

$$I(\tau) = \int_{-T}^{T} dt \, \left| E(t) + E(t+\tau) \right|^4$$

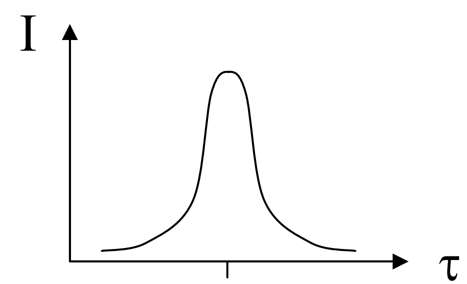

Useful for measuring rms duration of pulse

Two-frequency correlation function

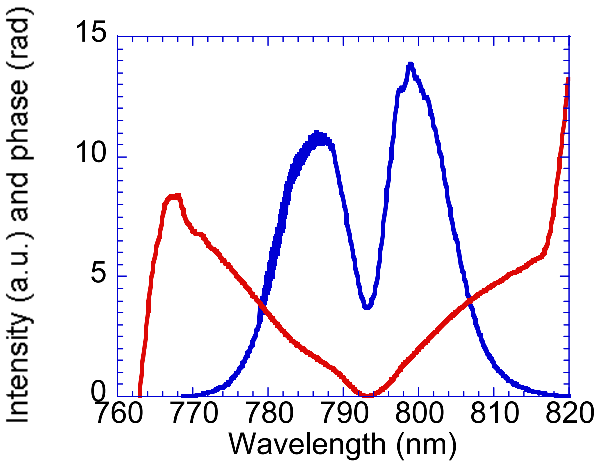

- Represent pulse by amplitude and phase of complex analytic signal

- Or more generally the two-frequency correlation function

$$C(\omega,\omega') = \left\langle \left\langle \tilde{E}(\omega-\omega_0)\tilde{E}^*(\omega'-\omega_0) \right\rangle \right\rangle$$

$C(\omega,\omega')$

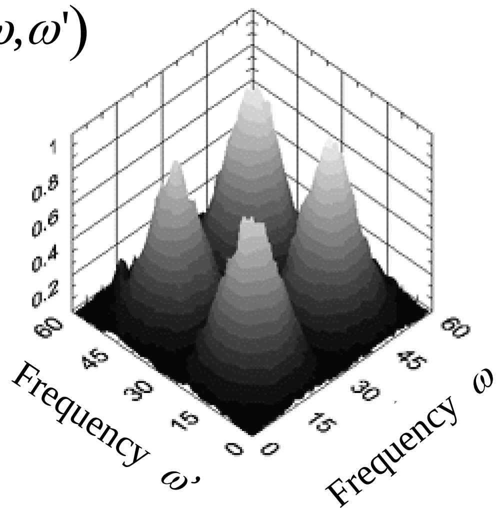

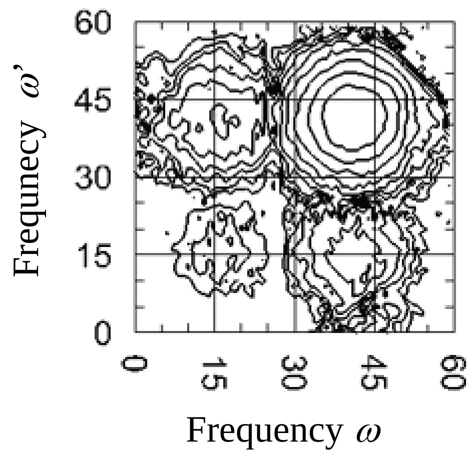

Useful for describing:

The properties of a pulse ensemble

All measurement strategies

Phase-space quasi-probability distributions

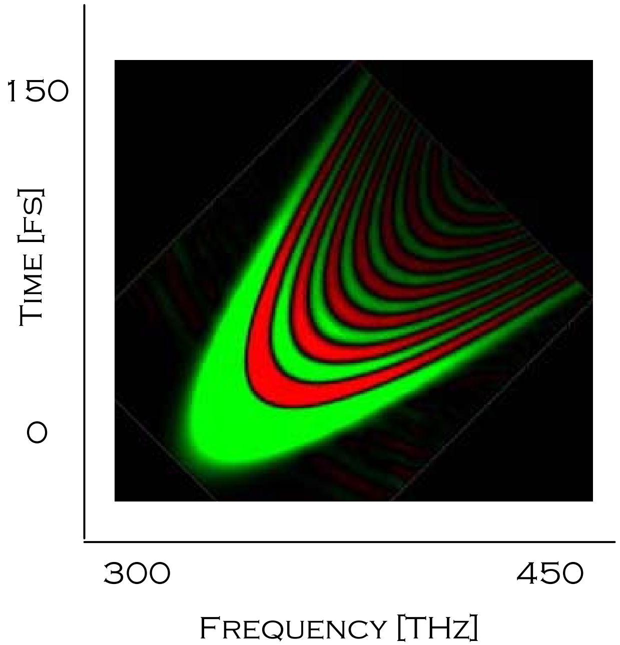

In the coherent (and near coherent) limit, a pulse of light cannot be described by a probability distribution.

Rather a quasi-probability distribution must be used, e.g. Wigner function

$$W(t,\omega) = \int_{-\infty}^{\infty} dt' \; e^{i\omega t'} \tilde{E}^*(t - t'/2)\tilde{E}(t + t'/2)$$

All measurements are overlaps of the Wigner function of the pulse ensemble with an apparatus function.

e.g. Gabor spectrogram

$$S(t,\omega) = \left| \int E(t') g(t'-t) \exp(i\omega t') dt' \right|^2$$

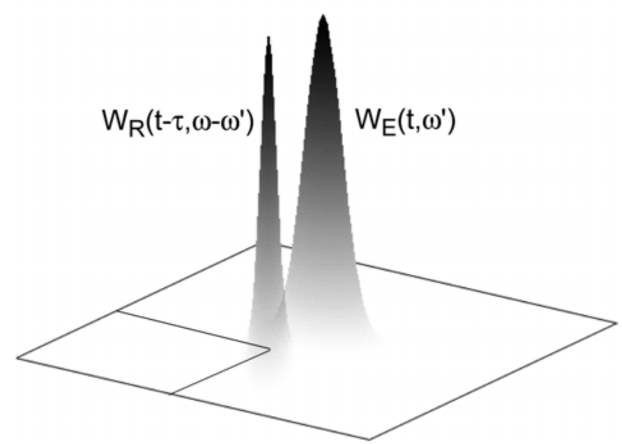

$$S(t,\omega) = W(t,\omega) \otimes \otimes W_{GATE}(t,\omega)$$

Phase space

Geometrical optics:

Ray transverse position (y)
Ray direction (u) (transverse wavevector)

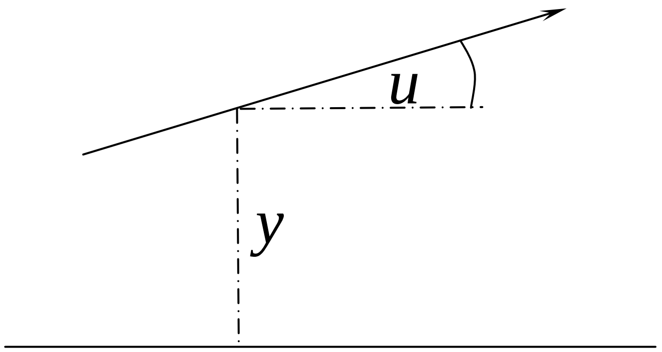

Geometrical optics phase space:

Each ray described by a point ($y.u$)
Ray bundles by a *phase-space probability distribution*

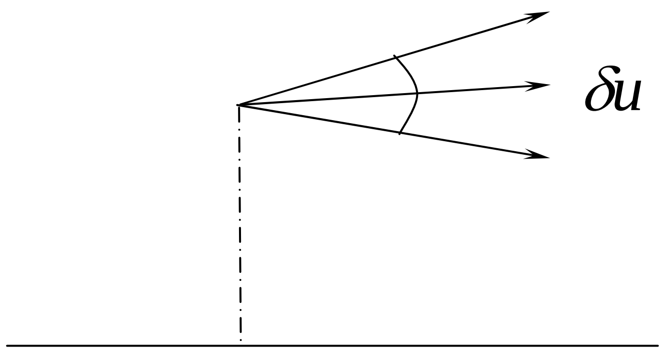

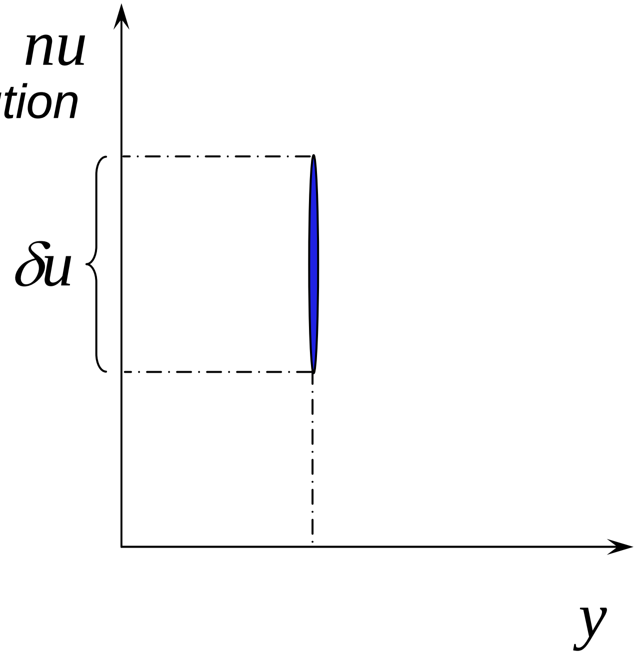

Action of linear optical elements in phase space

Free space propagation:

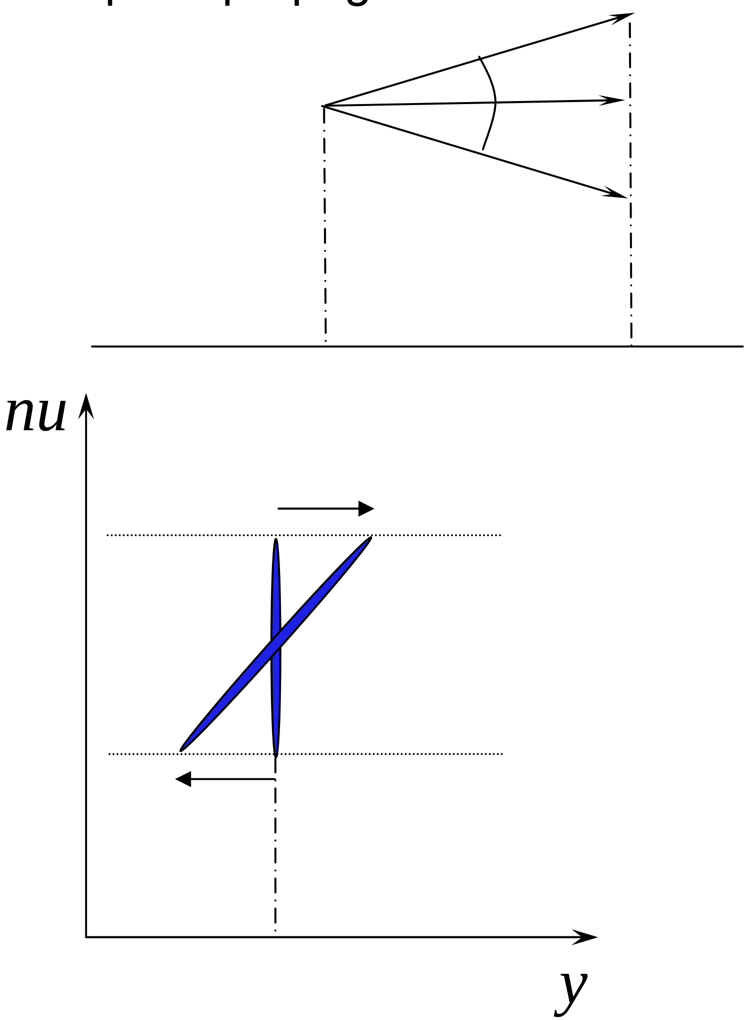

Paraxial lens:

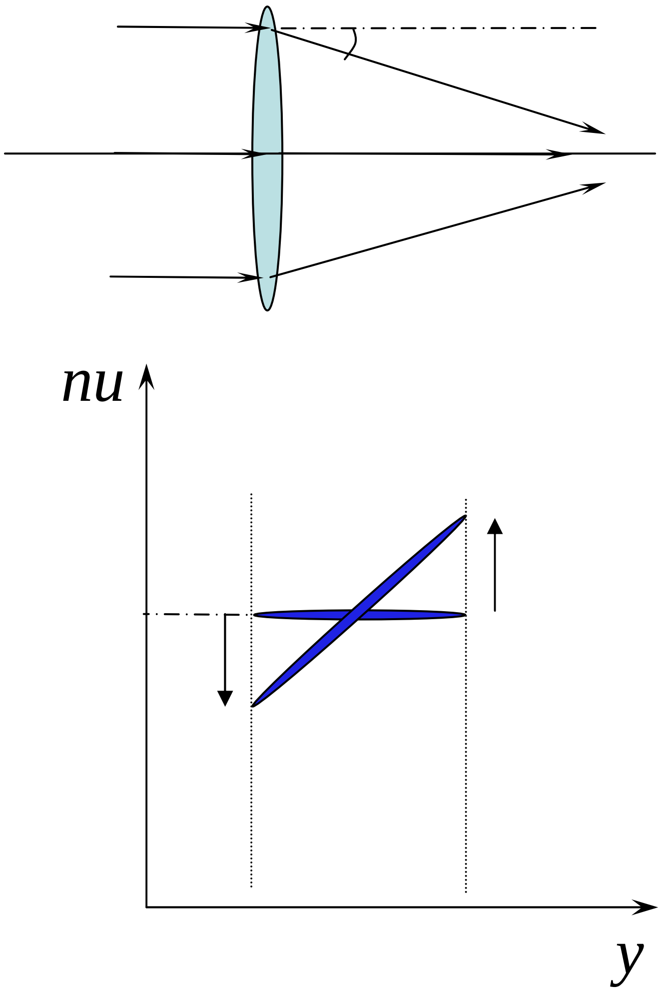

Chronocyclic phase space

Ultrafast optics: Pulse frequency (ω) & Pulse time of occurence (τ) $\underline{\Omega} = \begin{pmatrix} \omega \\ t \end{pmatrix}$

$\underline{\Omega}_{out} = \underline{\underline{T}}\,\underline{\Omega}_{in}$

$\tilde{E}_{out}(\omega) = e^{i\varphi_\omega''\omega^2}\tilde{E}_{in}(\omega)$

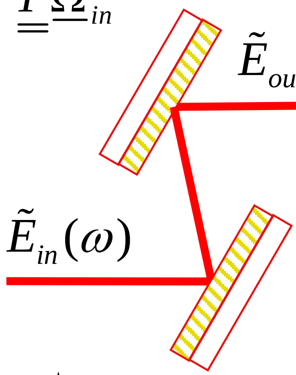

$\underline{\underline{T}}_{disp} = \begin{pmatrix} 1 & \varphi_\omega'' \\ 0 & 1 \end{pmatrix}$

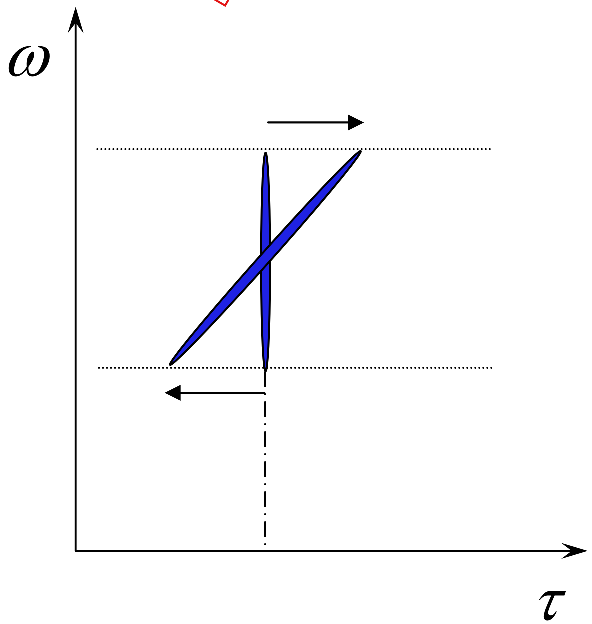

$E_{in}(t)$ $E_{out}(t) = e^{i\phi_t''t^2}E_{in}(t)$

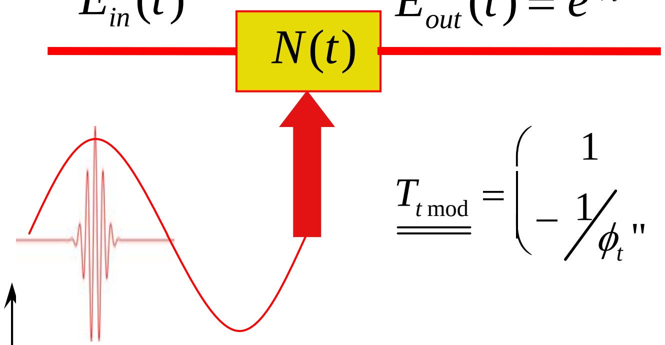

$\underline{\underline{T}}_{t\,mod} = \begin{pmatrix} 1 & 0 \\ -1/\phi_t'' & 1 \end{pmatrix}$

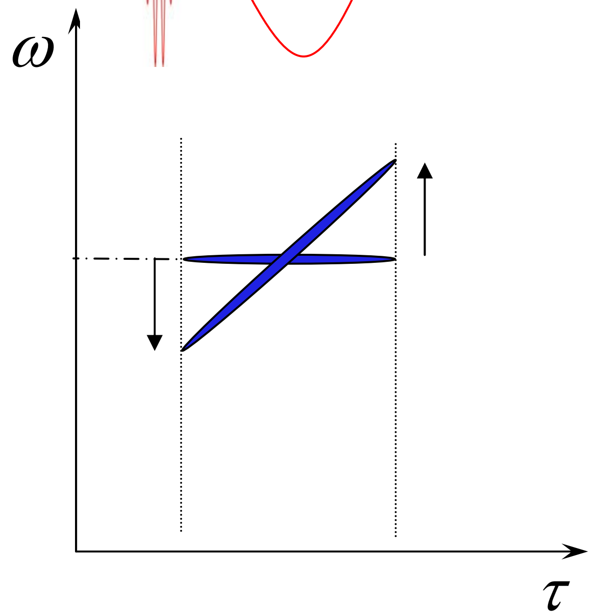

Nonlinear spectrography

*R. Trebino et al, Rev. Sci. Inst.., **23**, 792 (1997)*

FROG *: Frequency-resolved optical gating*

Measure spectrum of a series of temporal slices of pulse

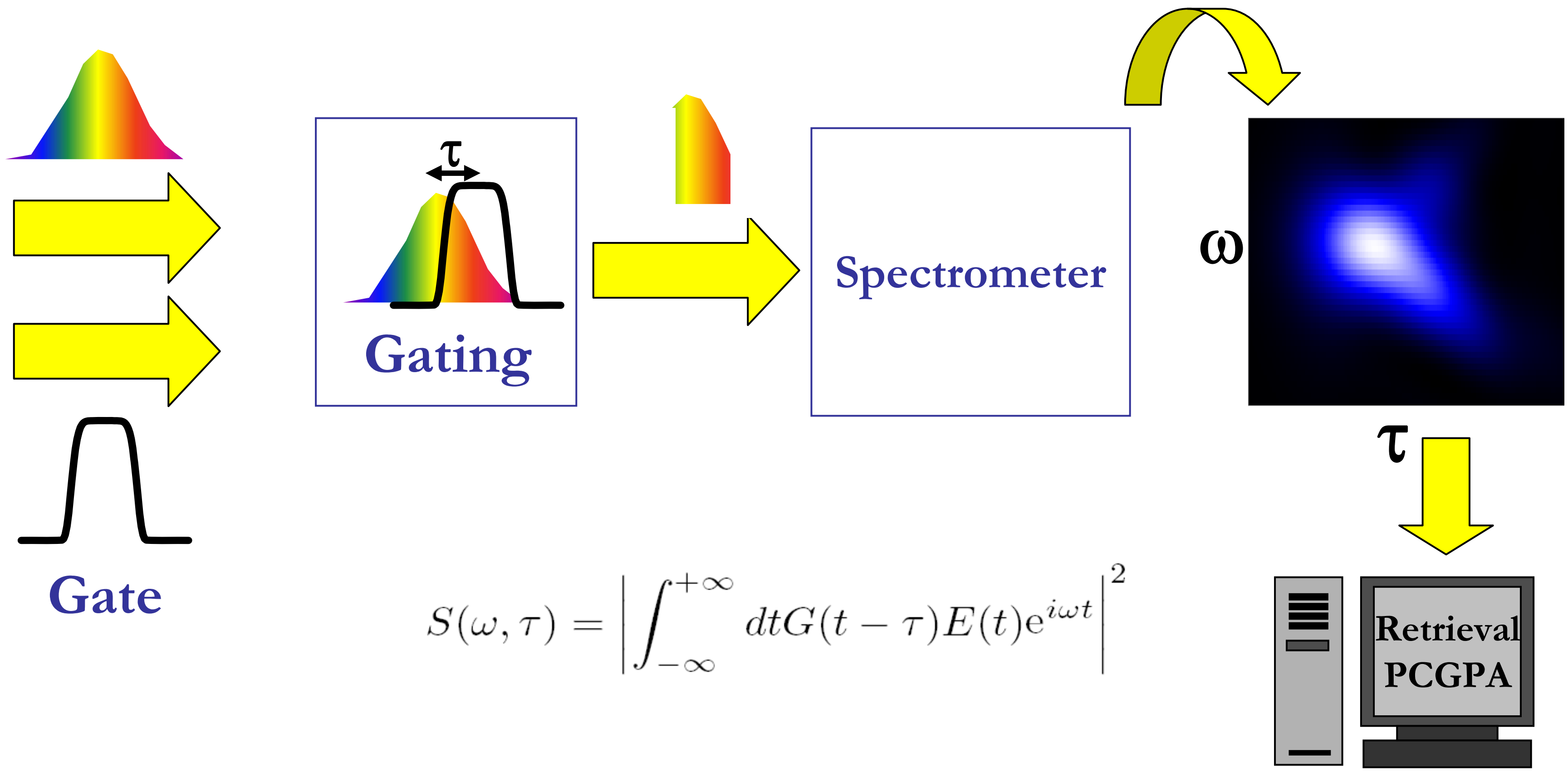

$$S(\omega,\tau) = \left| \int_{-\infty}^{+\infty} dt G(t-\tau) E(t) e^{i\omega t} \right|^2$$

Spectrography: inversion

Iterative reconstruction

Convex?

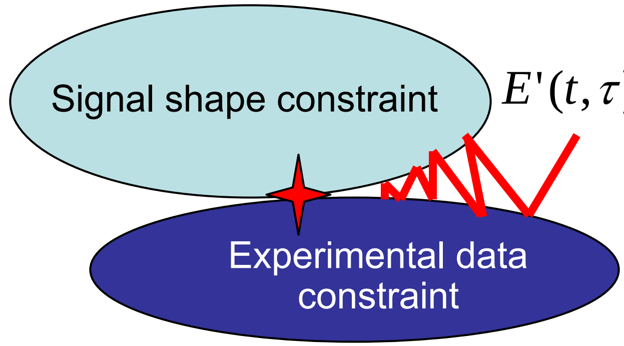

$$E'(t,\tau) = g(t,\tau)E(t)$$

$$I(\omega,\tau) = \left| \int_{-\infty}^{+\infty} E'(t,\tau)e^{-i\omega t}dt \right|^2$$

Calculate using I — Fourier transform — Replace modulus using II

$$E_n(t) \Rightarrow E_n'(t,\tau) = g_n(t,\tau)E_n(t) \Rightarrow S_n(\omega,\tau) = \int_{-\infty}^{+\infty} E_n'(t,\tau)e^{-i\omega t}dt \Rightarrow S_{n+1}(\omega,\tau)$$

Get new estimate using a projection algorithm

Current algorithm : Principal Component Generalized Projections (PCGP)

(*Kane, IEEE J.Q.E.,* ***35****, 421 (1999)*)

Field retrieval at 2 Hz

Complete characterization

Spectral shearing interferometry

*IAW and V. Wong, Opt. Lett., **19**, 287 (1994); C. Iaconis and I. Walmsley, Opt. Lett., **23**, 792 (1998)*

SPIDER *: Spectral Phase Interferometry for Direct E-field Reconstruction*

Measure spectral interference of pulse with a frequency-shifted replica

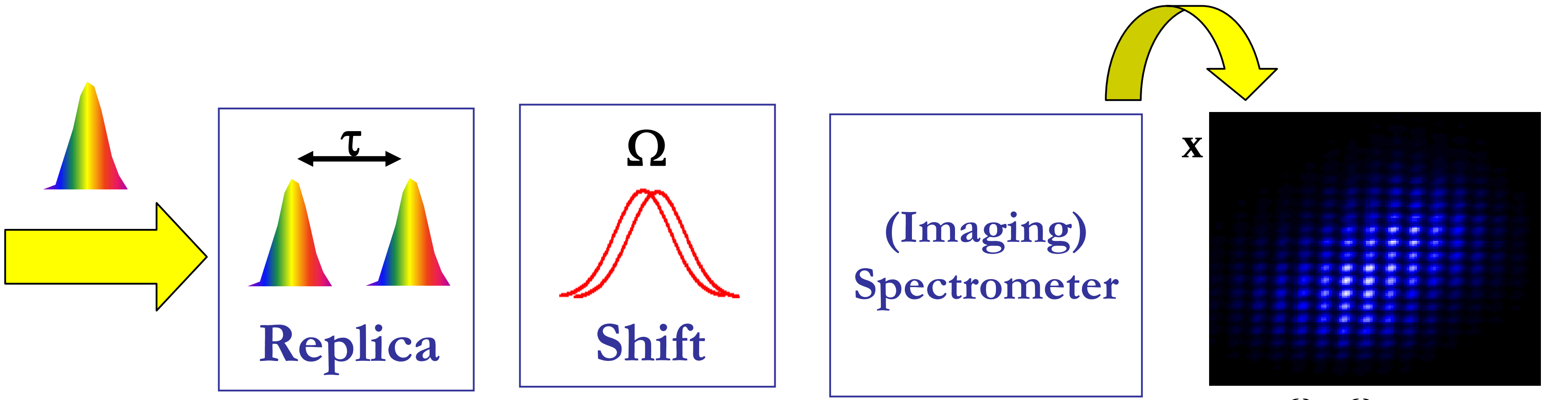

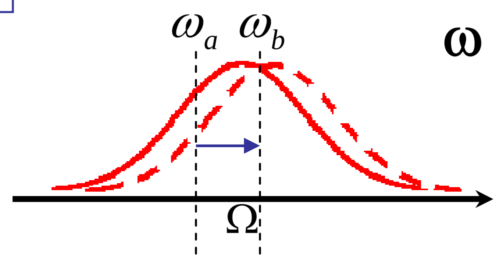

$$S(\omega;\tau) = \left|\tilde{E}(\omega-\omega_0) + \tilde{E}_R(\omega-\omega_0-\Omega)\exp(i\omega\tau)\right|^2$$

$$\varphi(\omega_b) - \varphi'(\omega_b) = \varphi(\omega_b) - \varphi(\omega_a)$$

Interferometry: inversion

Direct (algebraic) reconstruction

Low sensitivity to noise and detector spectral response

Measure interferogram and spectrum

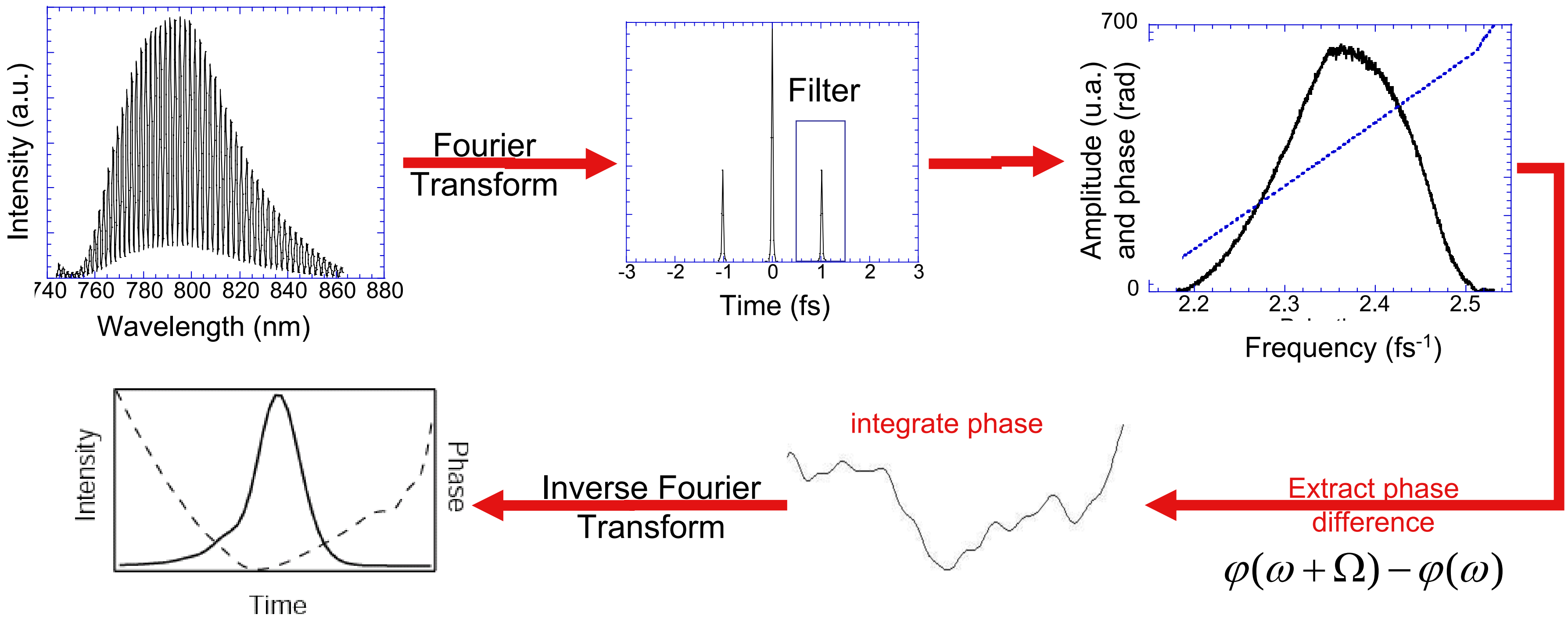

Complete characterization

Field retrieval at 1 kHz

(W. Kornelis et al, Opt. Lett. (2004))

Summary of methods

Possible approaches to complete pulse characterization

Second-order autocorrelations → Do not retrieve the electric field

Intensity autocorrelator (IAC) (1967)

Spectrographic techniques → 2D experimental trace

Iterative algorithms

Nonlinear spectrography (FROG) (1993)

Interferometric techniques → ID experimental trace

Direct (noniterative) algorithms

Nonlinear SSI (SPIDER) (1998)

Attosecond measurements

Require non-stationary filters with response times comparable to the pulse duration.

Temporal Phase modulation $N(t) = e^{i\Phi \cos\omega t}$

$E(t)$ $E_o(t) = e^{i\Omega t} E(t)$

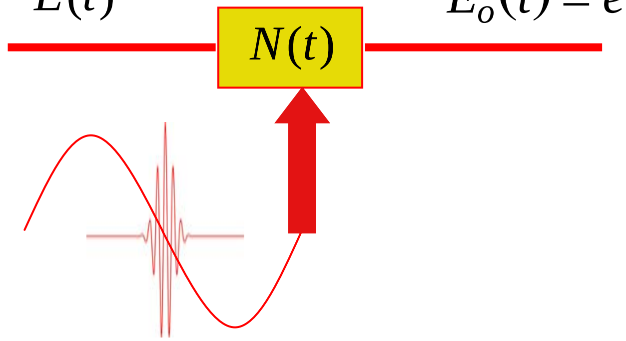

Linear phase modulation

Frequency shift

$E(t)$ $E_o(t) = e^{i\vartheta t^2} E(t)$

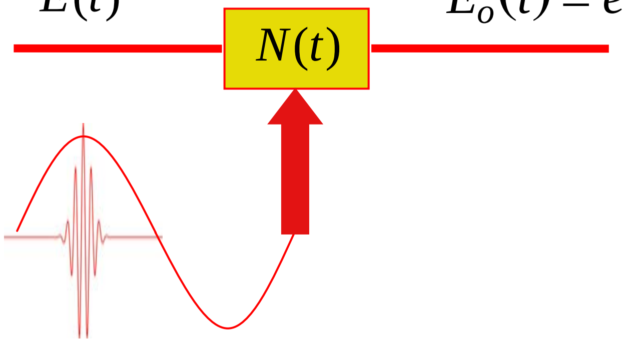

Quadratic phase modulation

Frequency chirp

For femtosecond pulses, it is usually necessary to use nonlinear optics

Temporal amplitude modulation

e.g. frequency doubling

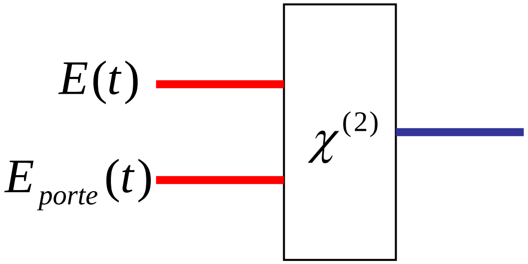

$$E'(t) = \chi^{(2)} E_{gate}(t) E(t)$$

Temporal phase modulation

e.g. cross phase modulation

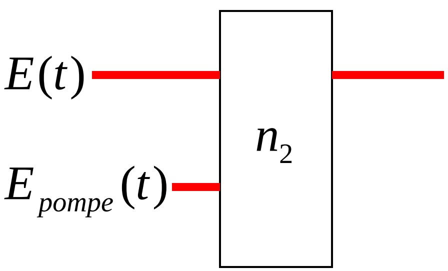

$$E'(t) = \exp(i\alpha I_{pump}(t)) E(t)$$

$S \propto |E|^4$ ou $|E|^6$ ⇒ Loss of sensitivity compared to the use of a reference pulse

The filter is unknown ⇒ Reconstruction may be complicated

Outline

SPIDER

Spectral Phase Interferometry for Direct Electric-field Reconstruction (SPIDER)

Self-referencing spectral shearing interferometry

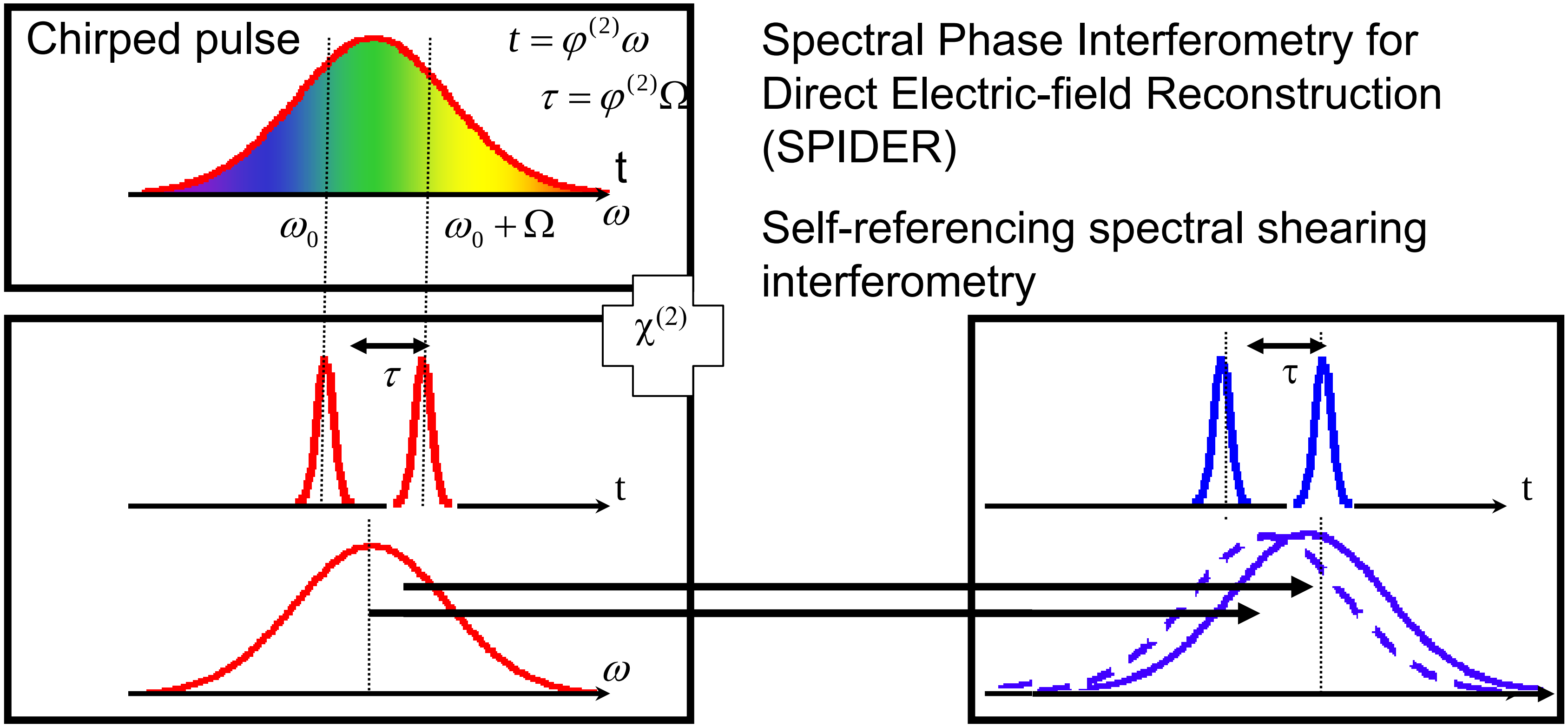

Spectral interferometry : $\varphi(\omega-\omega_0)-\varphi(\omega-\omega_0-\Omega)+\omega\tau$

$\varphi(\omega+\Omega)-\varphi(\omega)$

$\varphi(\omega)$
$I(\omega)$
} Complete characterization

*C. Iaconis and I. Walmsley, Opt. Lett., **23**, 792 (199*

Spatially resolved SPIDER

Gallman et al. Opt. Lett., 26, 96 (2001)

Non-linear interaction

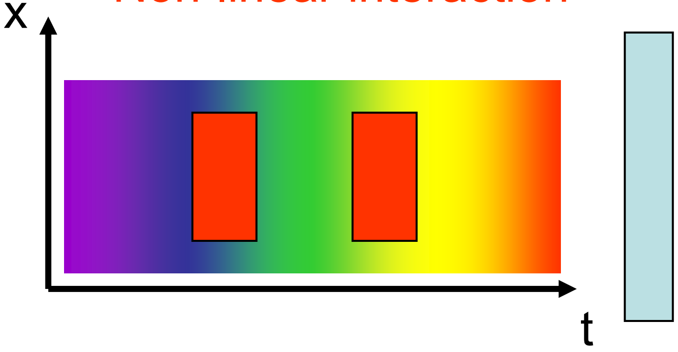

Interaction with plane waves at ω_0 and $\omega+\Omega$

$$\tilde{E}(x,\omega-\omega_0)$$
$$\tilde{E}(x,\omega-\omega_0-\Omega)$$

For non-planar wavefronts

$$\tilde{E}(x,\omega-\omega_0)\exp(i\varphi(x,\omega_0))$$
$$\tilde{E}(x,\omega-\omega_0-\Omega)\exp(i\varphi(x,\omega_0+\Omega)$$

(can still reconstruct ϕ using the spatial gradient)

Interferogram acquisition using a 2-d spectrometer

$$\left|\tilde{E}(x,\omega-\omega_0)+\tilde{E}(x,\omega-\omega_0-\Omega)\exp(i\omega\tau)\right|^2$$

$$\varphi(x,\omega+\Omega)-\varphi(x,\omega)=\Omega\boxed{\frac{\partial\varphi}{\partial\omega}(x,\omega)}$$

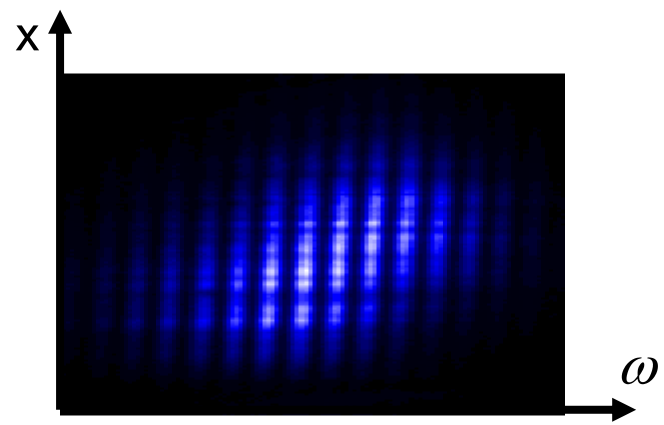

Spectrally resolved lateral shearing interferometry

Shearing interferometry in the (x,ω) domain

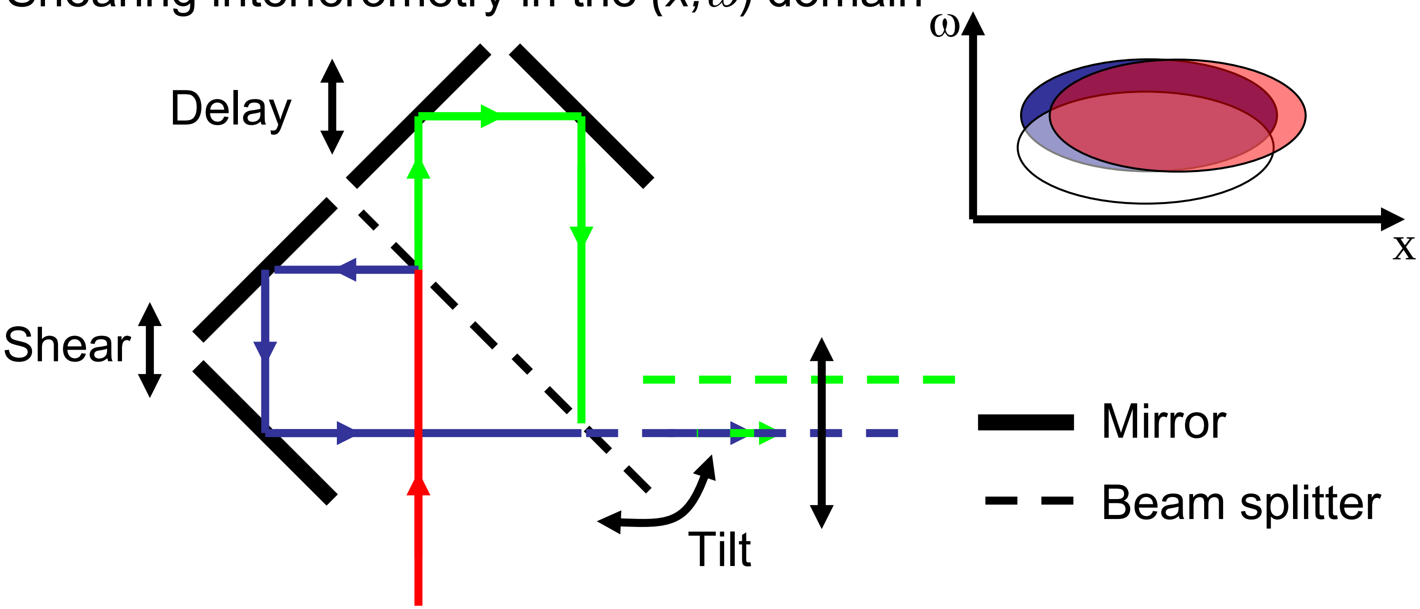

$$\frac{\partial \varphi}{\partial x}(x,\omega)$$

$$\frac{\partial \varphi}{\partial \omega}(x,\omega)$$

Acquisition with a 2-d spectrometer

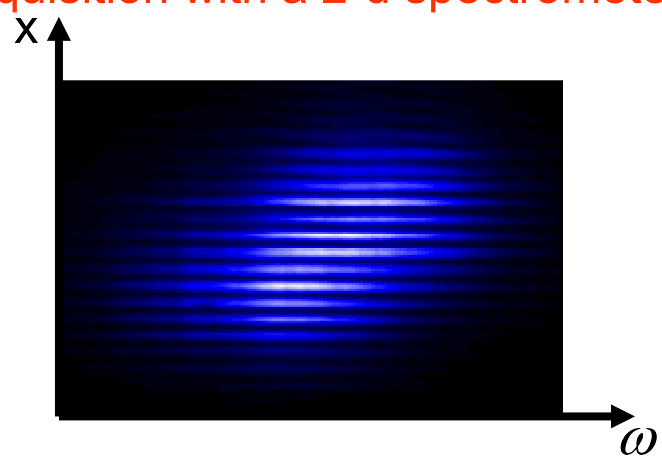

$$\left|E(x+X,\omega)+E(x,\omega)\exp(iKx)\right|^2$$

$$=> \varphi(x+X,\omega)-\varphi(x,\omega) = X\boxed{\frac{\partial \varphi}{\partial x}(x,\omega)}$$

Space-time SPIDER

Dorrer, Kosik and IAW Opt. Lett., 27, 548 (2002)

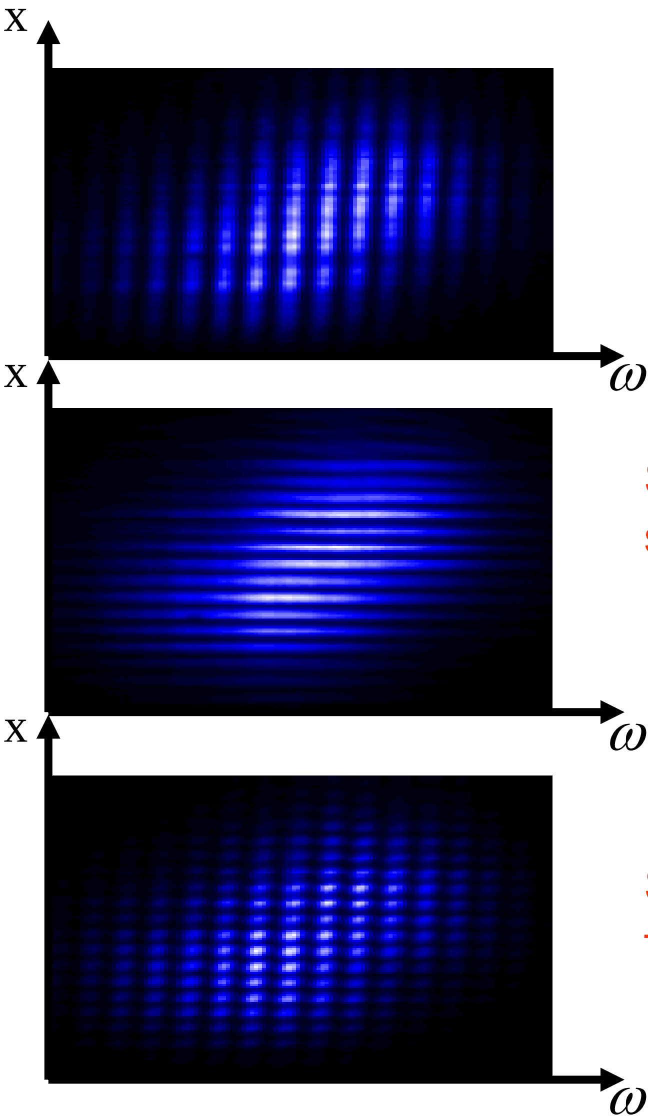

Spatially resolved SPIDER

Spectrally resolved shearing interferometry

Simultaneous measurement for single-shot operation

$$\frac{\partial \varphi}{\partial \omega}(x,\omega)$$

$$\frac{\partial \varphi}{\partial x}(x,\omega)$$

$$\rightarrow \varphi(x,\omega)$$

Complete space-time field characterization

Space-time coupling using ST-SPIDER

Characterization of pulse with angular dispersion (pulse-front tilt)

$$\frac{\partial\theta}{\partial\lambda}$$

$$\tilde{E}'(\omega,k)=\tilde{E}(\omega,k-\gamma\omega)$$
$$\tilde{E}'(\omega,x)=\tilde{E}(\omega,x)\exp(i\gamma\omega x)$$
$$\tilde{E}'(t,x)=\tilde{E}(t-\gamma x,x)$$

Spatio-spectral **phase** after an LaK21 prism

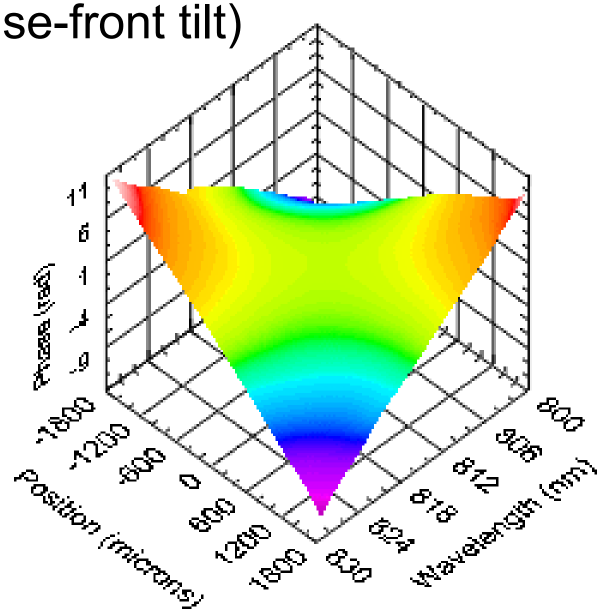

Pulse front tilt for 3 different prisms

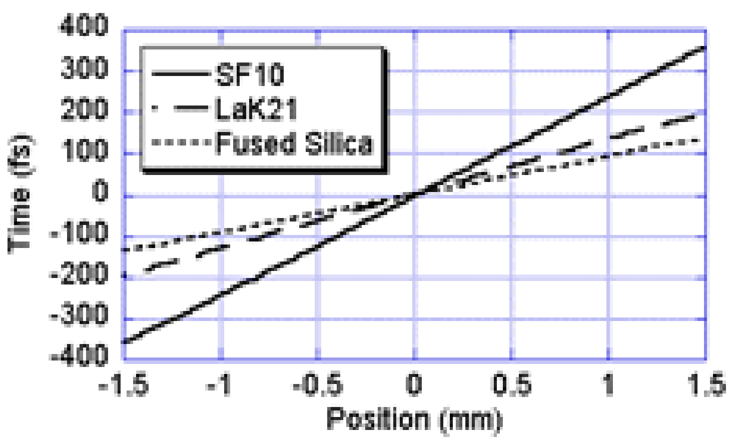

Space-time coupling coefficient

Prism	γ measured (fs.mm^{-1})	γ calculated (fs.mm^{-1})
Fused silica	91.5	90.8
LaK21	132.3	131.9
SF10	241.8	247.3

Pulse front tilt reconstructed using ST- SPIDER

Spatio-temporal **intensity** after an LaK21 prism

$$\tilde{E}'(t,x) = \tilde{E}(t-\gamma x, x)$$

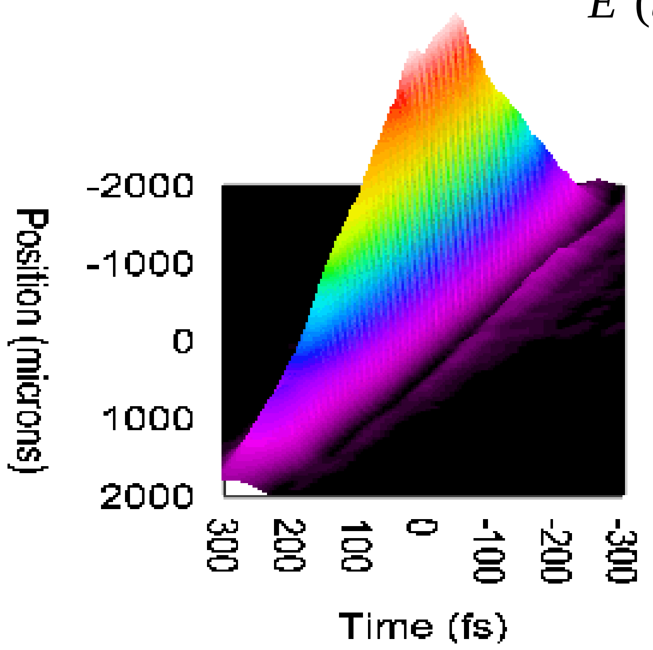

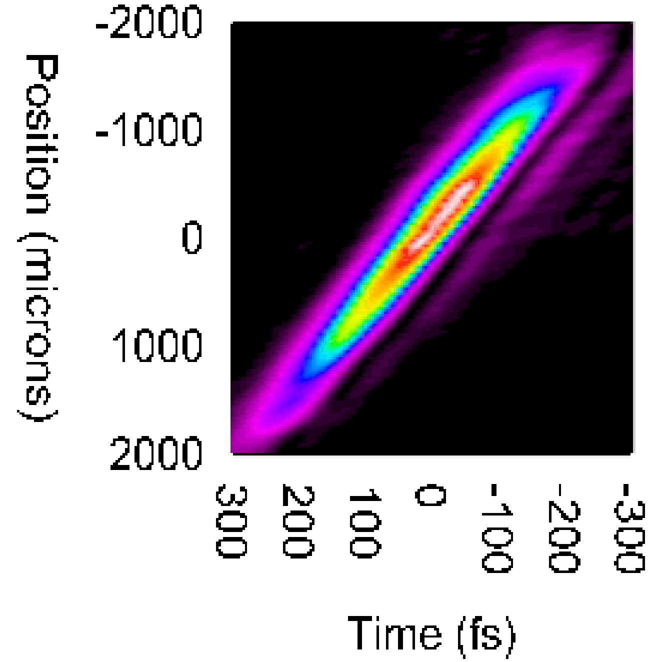

Precise measurement of space-time coupling constant
γ with no prior assumptions

Misaligned compressor using ST-SPIDER

Misaligned compressor leads to space-time coupling in the *x* and *y* directions

Optimization of the spatio-temporal electric field in these two directions

Before

$\gamma_X = 14 \ fs.mm^{-1}$

$\gamma_Y = 63 \ fs.mm^{-1}$

After

$\gamma_X = 0.7 \ fs.mm^{-1}$

$\gamma_Y = -0.5 \ fs.mm^{-1}$

Plot of data set $I(x,y,t) \geq \frac{1}{2} I_{MAX}$

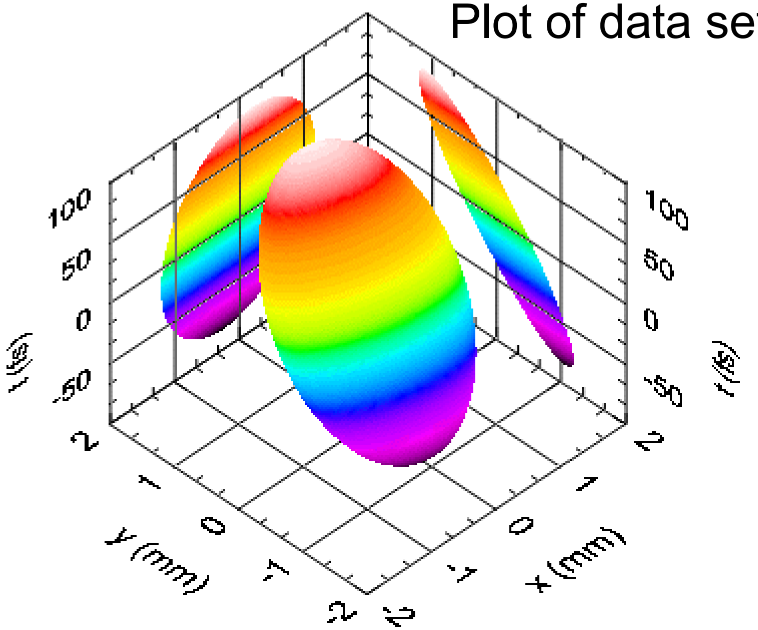

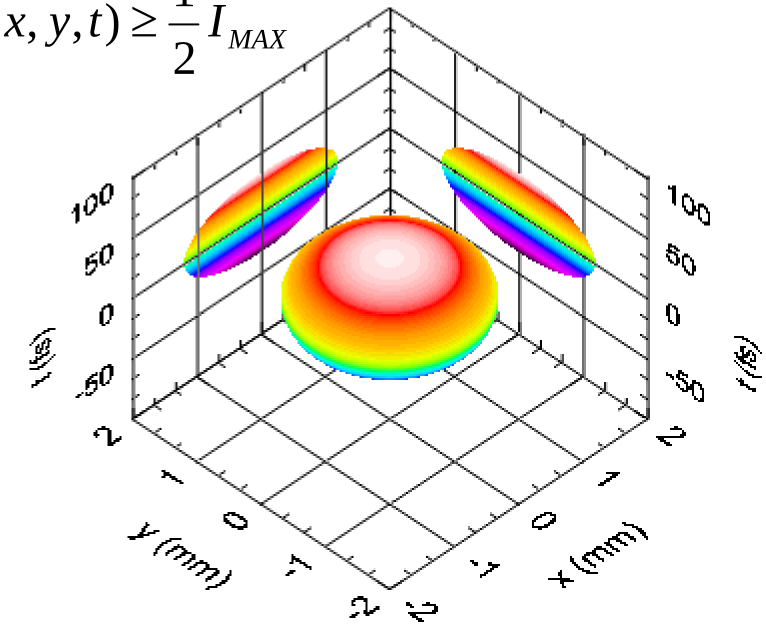

Nonlinear phase characterization

Collaboration with
R. W. Boyd and G. Piredda
Univ. Of Rochester

Spatio-spectral phase at high energy

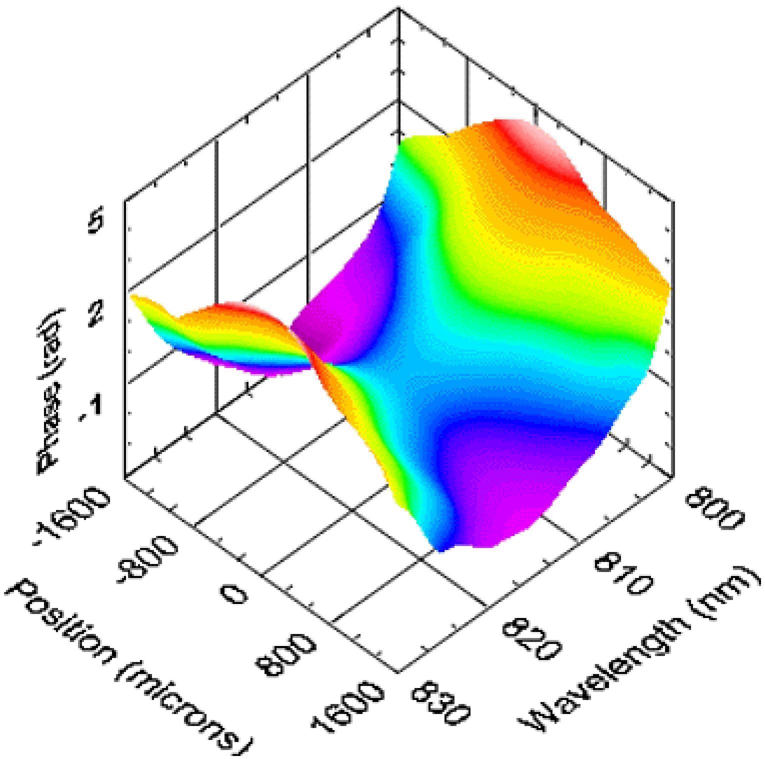

Spatial phase at t=0

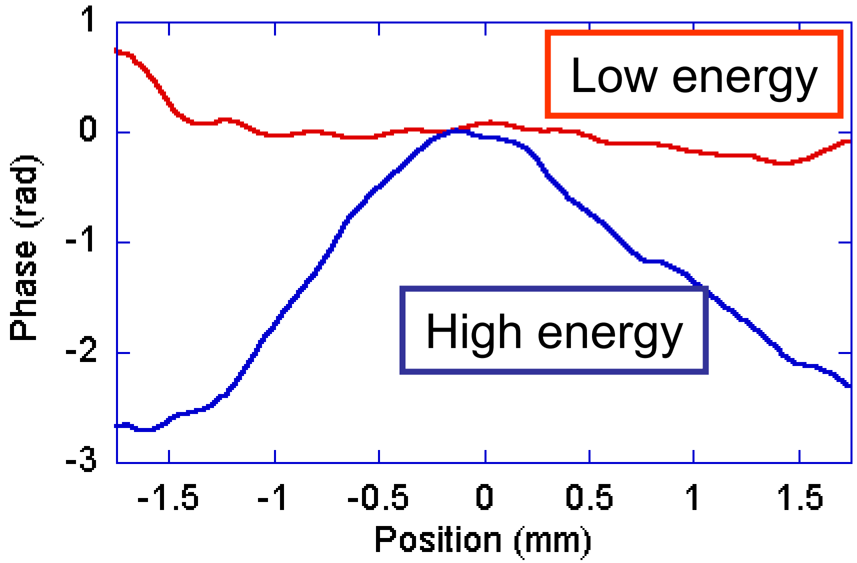

SPIDER features

Features:

High sensitivity

Good SNR - single shot operation

Algebraic phase reconstruction from measured signal

Provably unique solution

Rapid pulse-shape reconstruction

Robust reconstruction

Accuracy not dependent on detector response

Redundant data gives precision and consistency check

Inherent 2-D acquisition

Space-time characterization with no assumptions

SPIDER applications

Pulse characterization is an important topic for many areas: e.g. biomolecular optics

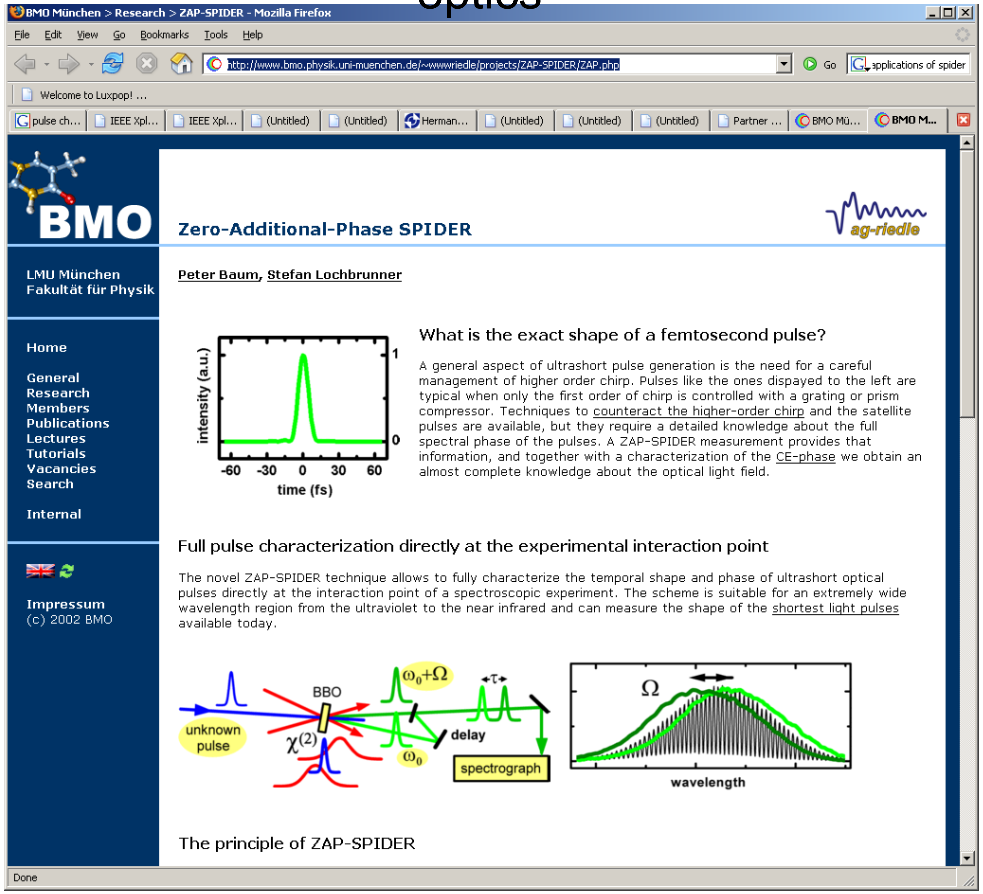

http://www.bmo.physik.uni-muenchen.de/~wwwriedle/projects/ZAP-SPIDER/ZAP.php

• *In situ* measurements for nonlinear microsopy

Characterization at the focus of a high-NA objective, using a Fourier-domain pulse shaper

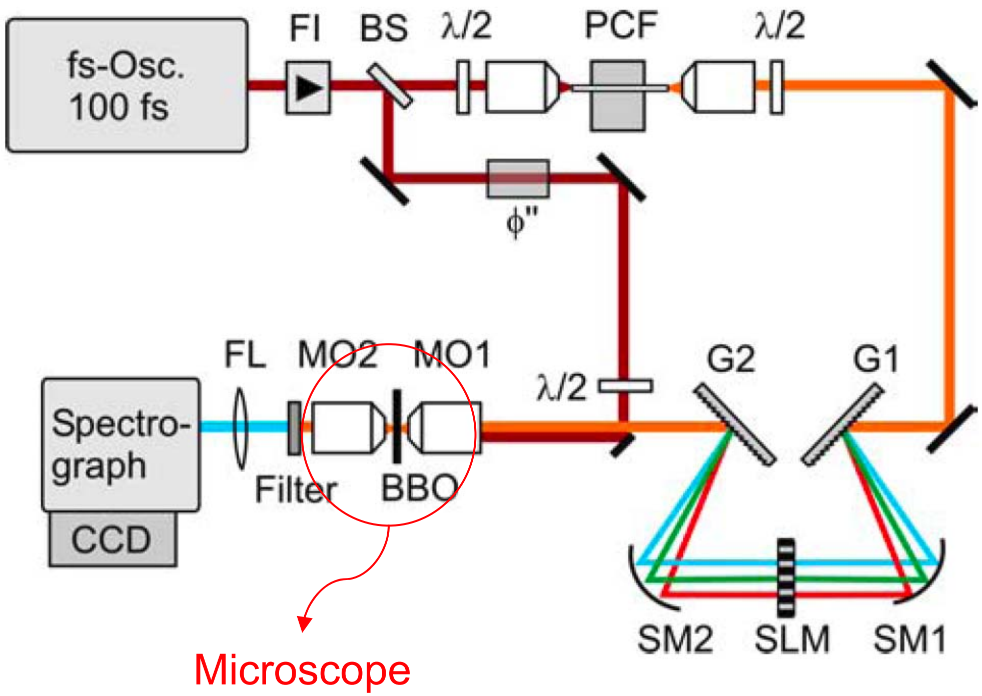

Prof. Dr. M. Motzkus, Marburg

SPIDER applications

- Real-time feedback control of shaped pulses

QuickTime™ and a
Microsoft Video 1 decompressor
are needed to see this picture.

Prof. M. E. Anderson, San Diego

SPIDER applications

- Dispersion management in telecommunications fiber links

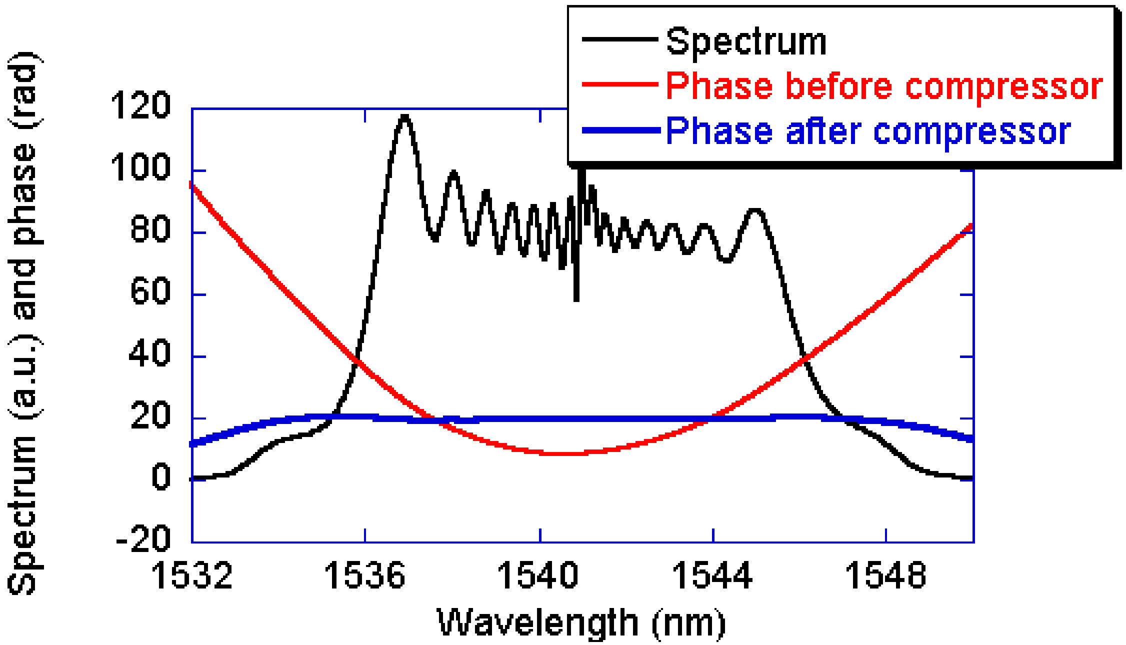

Dr. C. Dorrer, Lucent Technologies

SPIDER applications

- Few-cycle and octave-spanning pulses

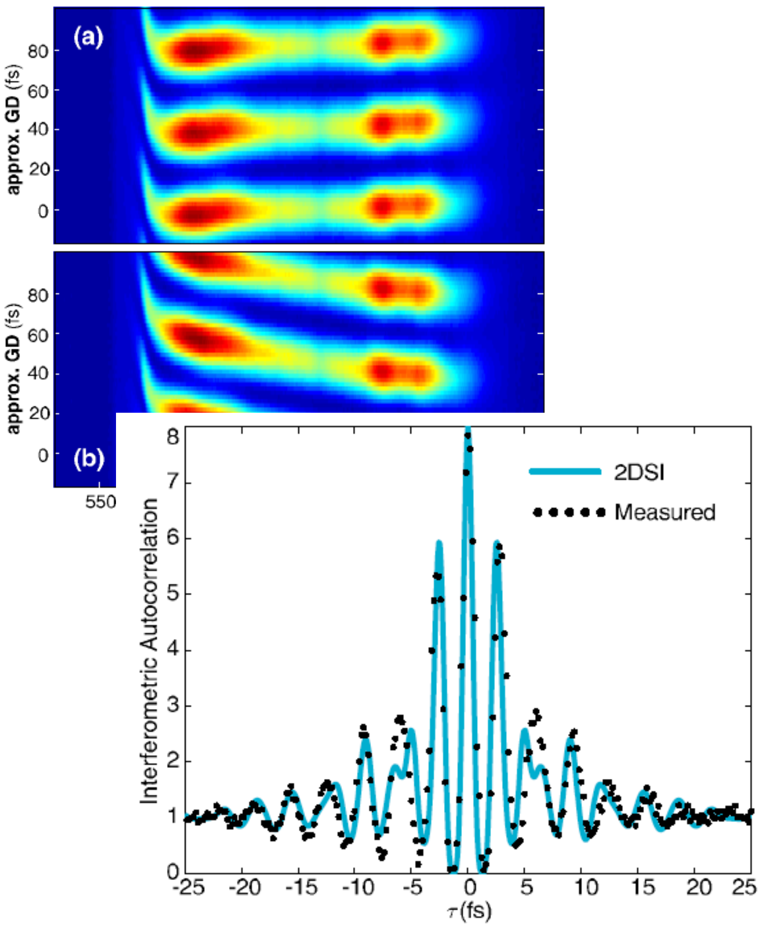

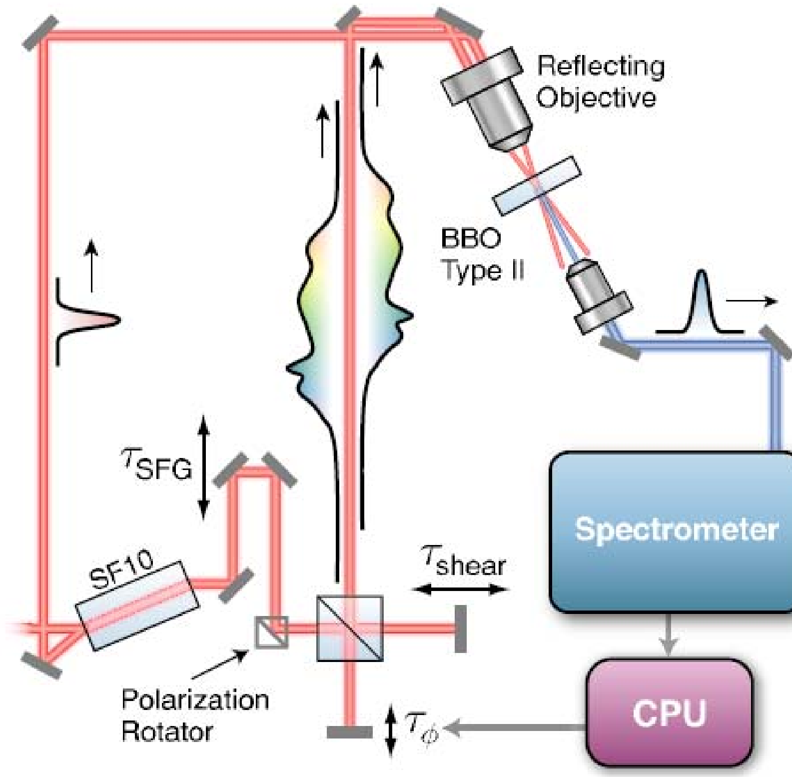

Prof. F. Kärtner, MIT

Commercialization

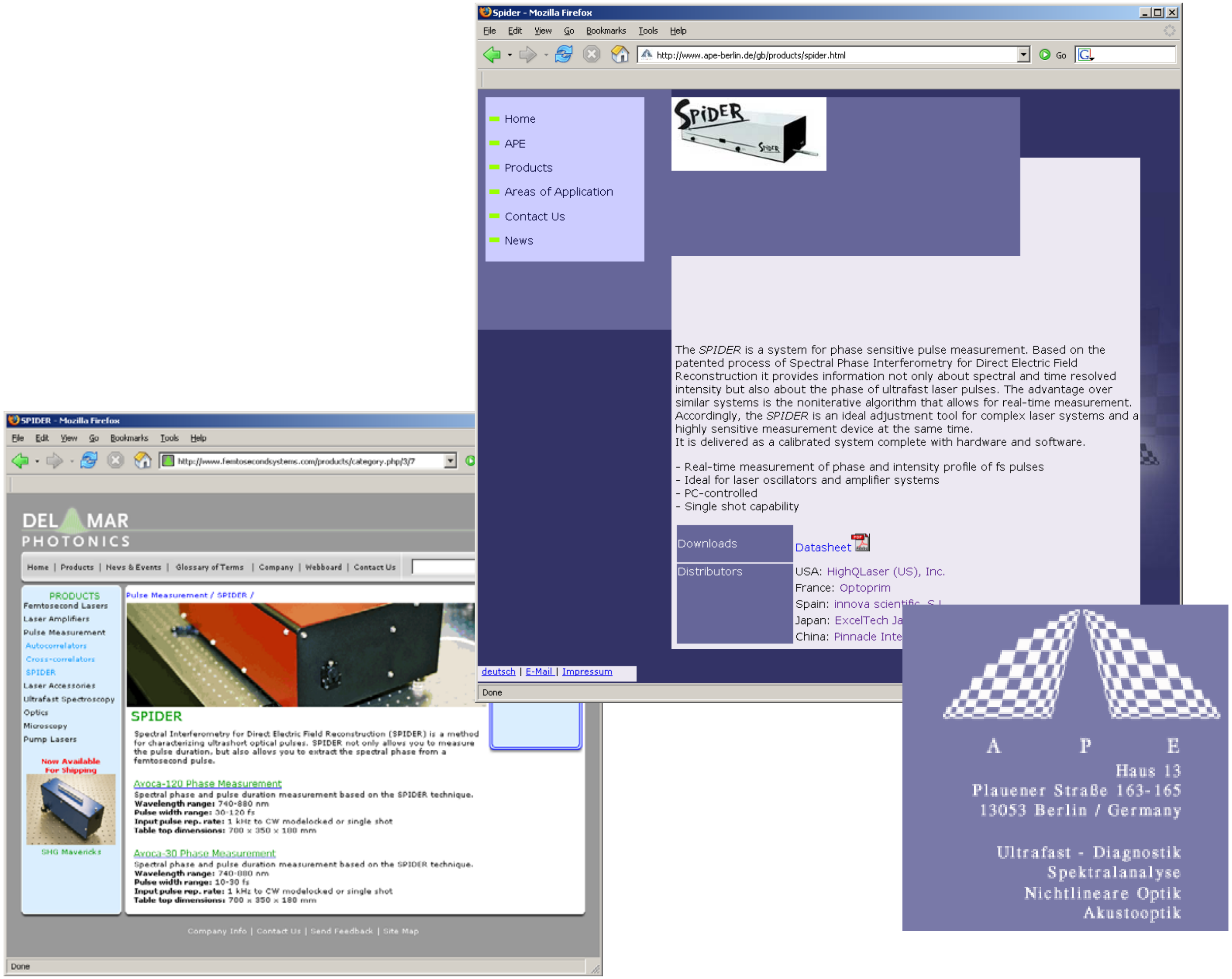

Outline

I . Introduction
II.General principles of pulse characterization
III. SPIDER
IV. Spatial coding
V. Long crystals
VI. Into the attosecond regime

SEA-SPIDER: spatial coding

- Spatial coding of spectral phase - optimal sampling of spectrum
- No replication of test pulse - suited for extreme bandwidths

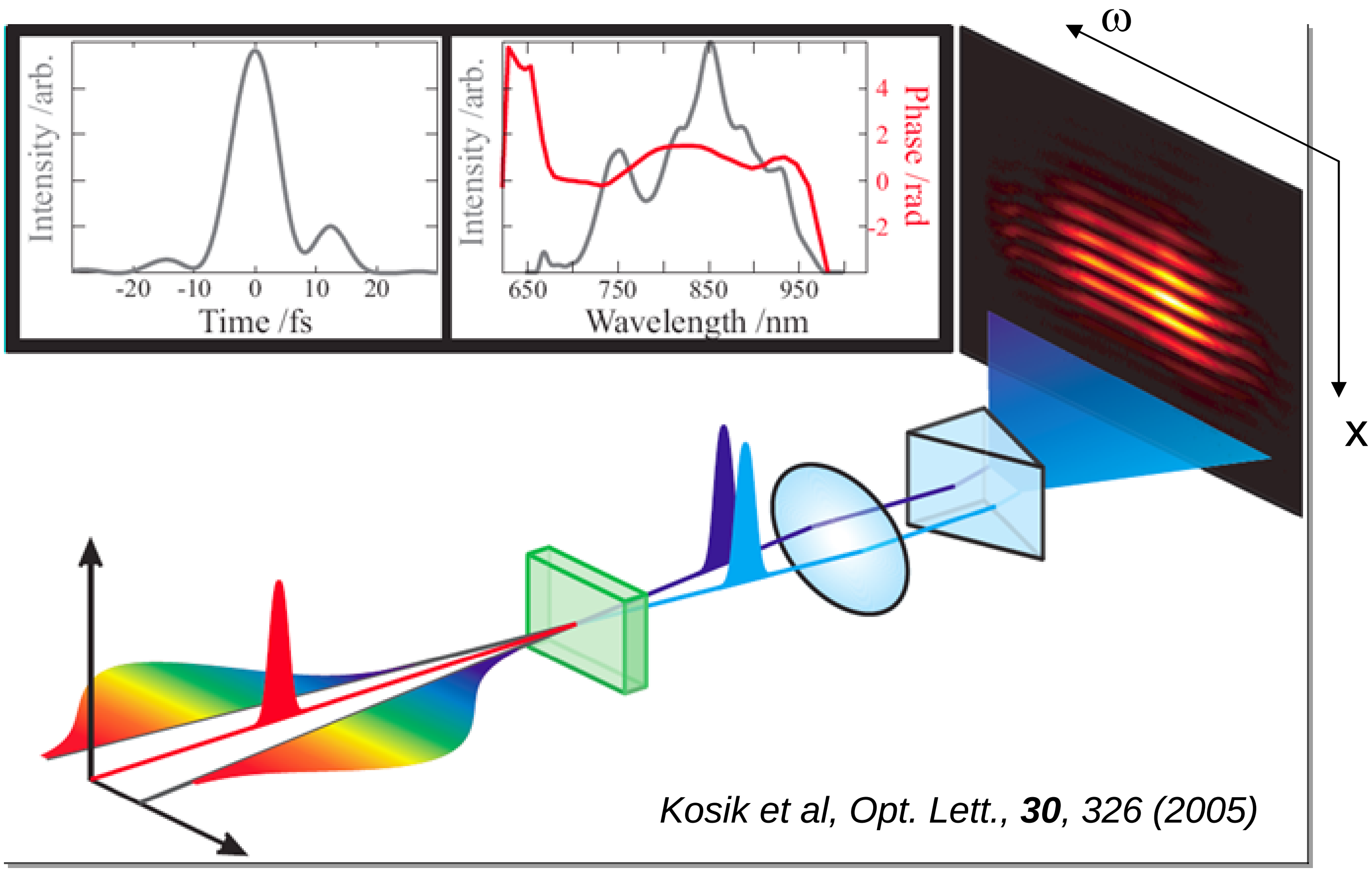

Spatial coding of spectral phase

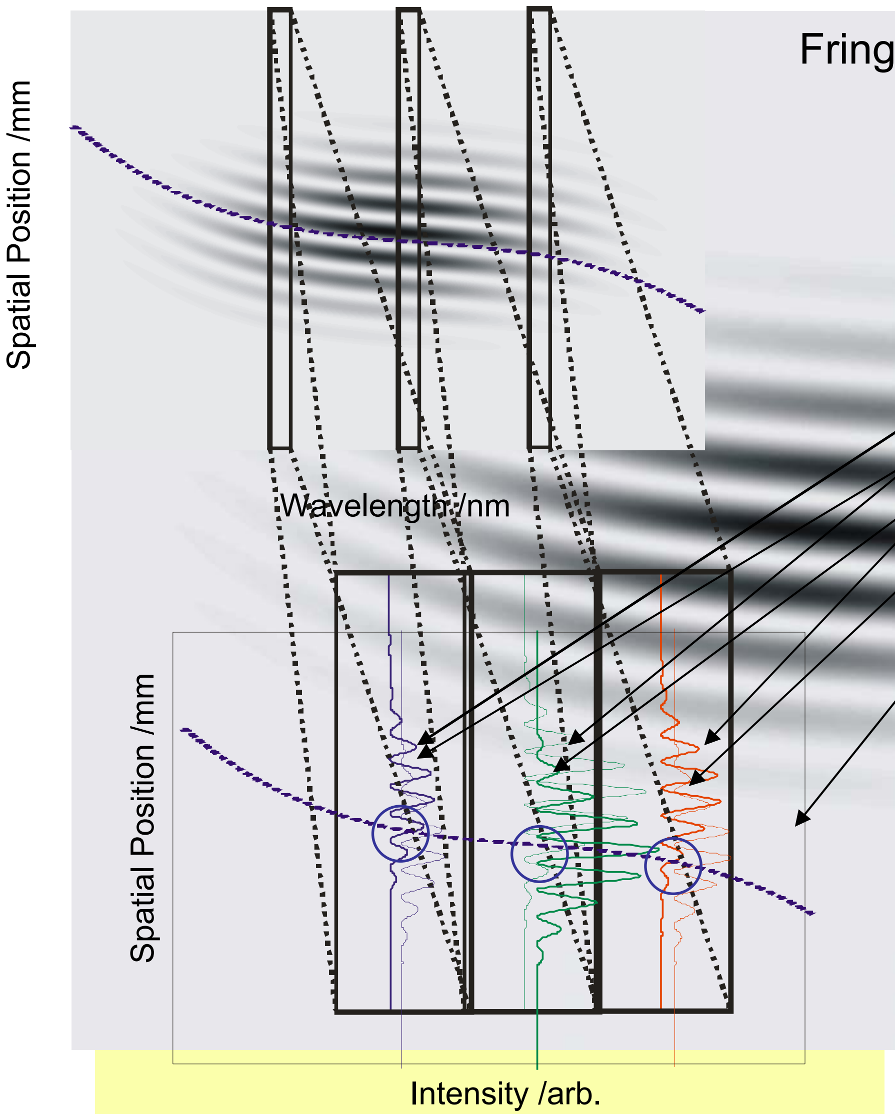

Fringe pattern given by:

$$I(\omega, x) \sim \cos\left[\frac{\partial \phi(\omega, x)}{\partial \omega} + Kx\right]$$
$$\sim \cos[Kx + \varphi(\omega)]$$

- Fringes due to tilt between beams.
- Fringe position due to spectral phase.
- Contours of fringe pattern directly map out spectral phase gradient.
- Space Time Coupling distorts fringe pattern
- Reconstruction performed by a fast Fourier transform filtering routine.

SEA-SPIDER apparatus for few-cycle pulses

Wyatt et al, Opt. Lett., ***31****, 914 (2006)*

Experimental implementation suitable for octave-spanning spectra

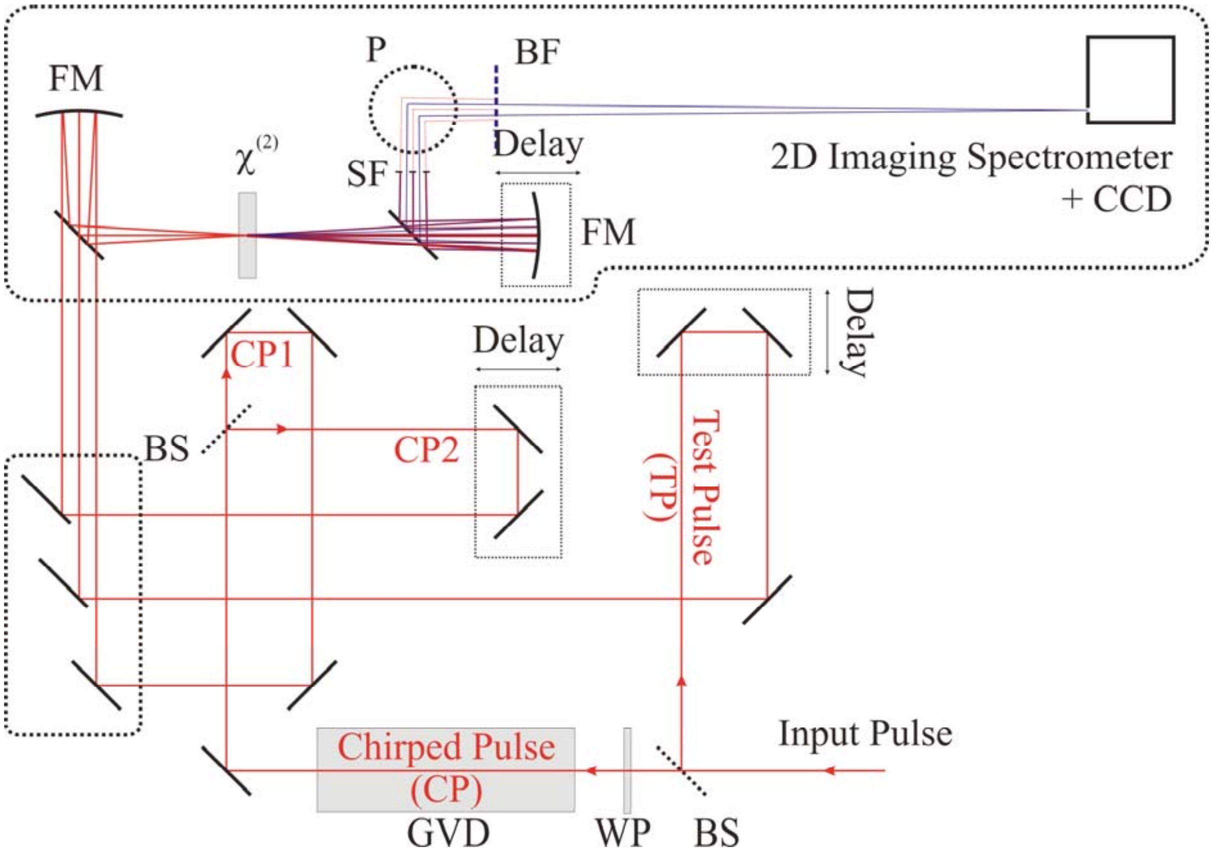

(Collaboration with Gero Stilbenz and Günter Steinmeyer, MBI, Berlin)

SEA-SPIDER for 6 fs HCF system

Pulses generated by self-phase modulation in Ar in a hollow-core fiber, with chirped-mirror compression

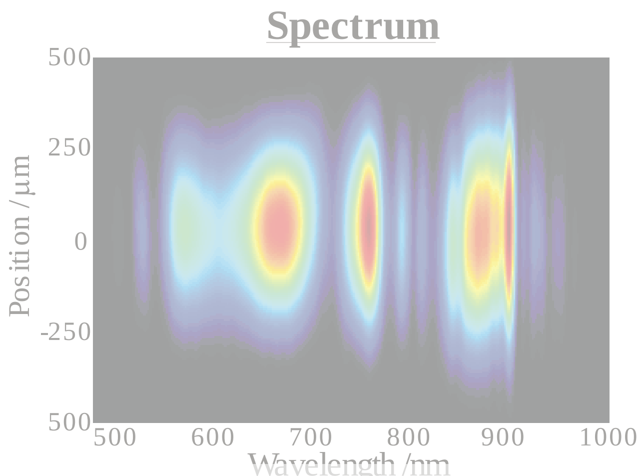

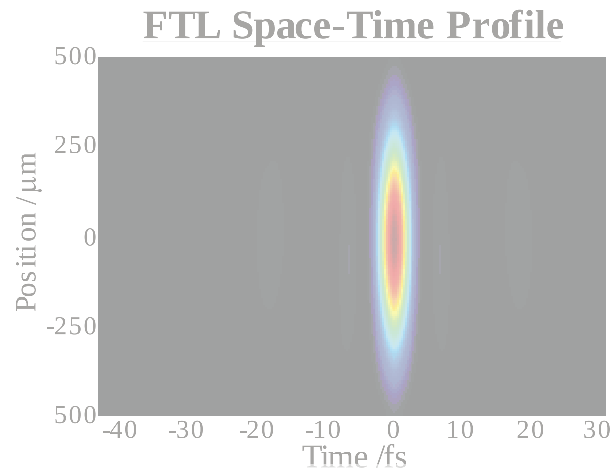

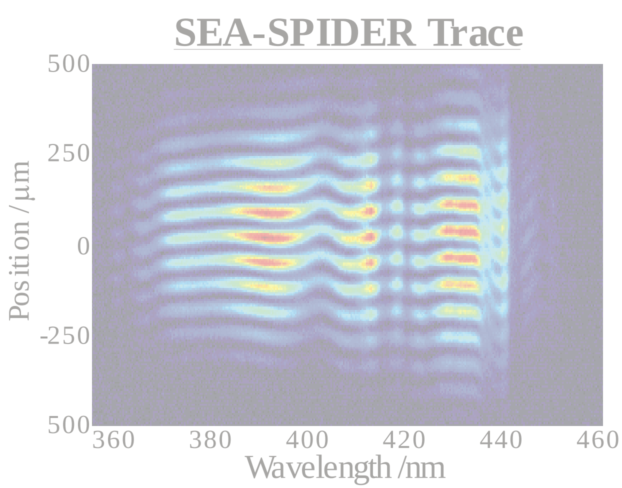

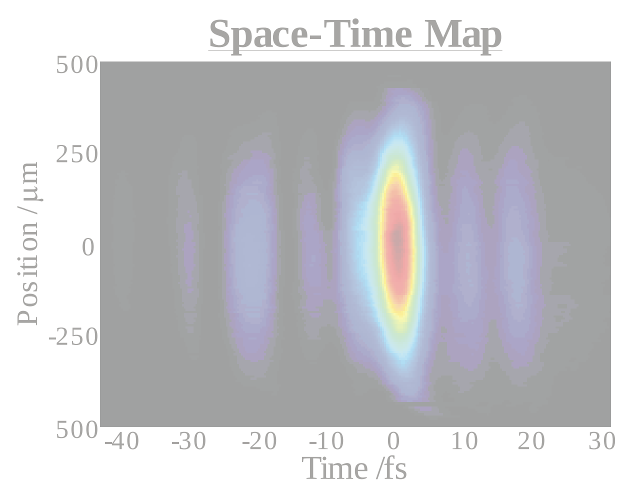

Outline

LX-SPIDER: long crystals for short pulses

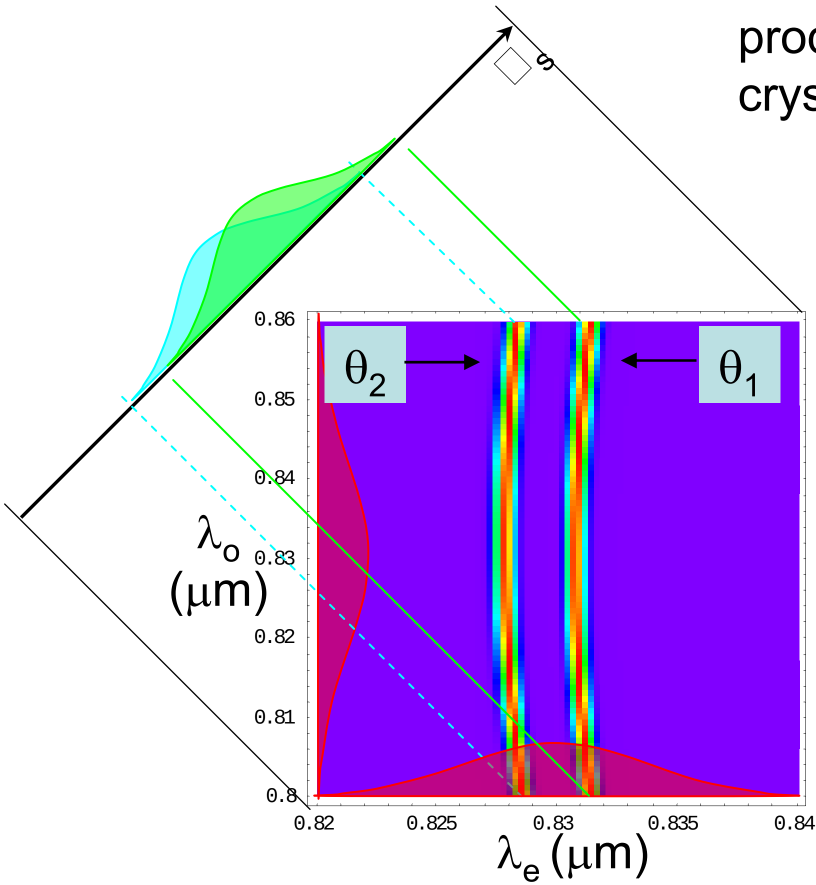

Type-II collinear SFG

Main idea: spectral shear can be directly produced in a suitably designed nonlinear crystal

$$\Delta k(\omega_1, \omega_2) = k_o(\omega_1) + k_e(\omega_2) - k_e(\omega_1 + \omega_2)$$

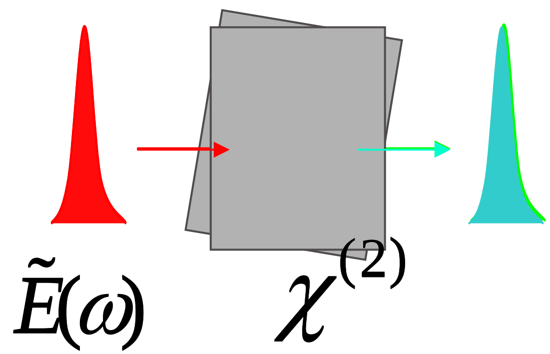

- Δk – PMF shape
  asymmetric group velocity matching
- L – PMF width

A.M. Weiner, *JQE* 19 (1983)

† W. P. Grice et. al., *PRA* 64 (2001)

LX-SPIDER: long crystals for short pulses

Radunsky, Kosik, IAW, Wasylczyk, Wasilewski, U'Ren and Anderson, Opt. Lett., 31, 1 (2006)

The spectral shear can be directly produced in a suitably designed extended three wave

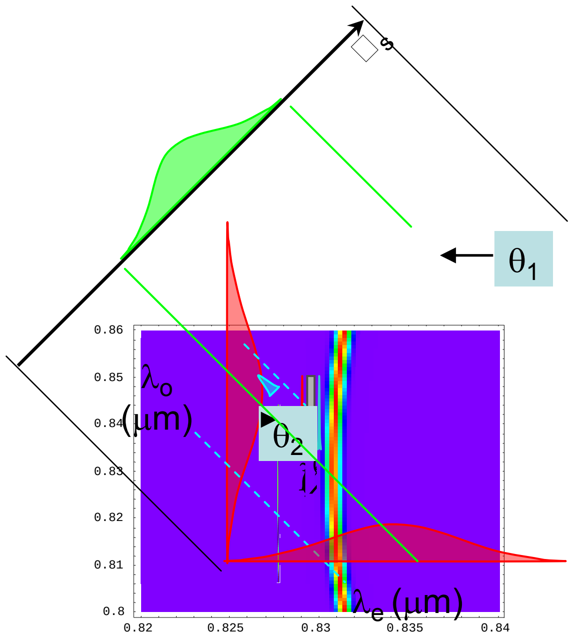

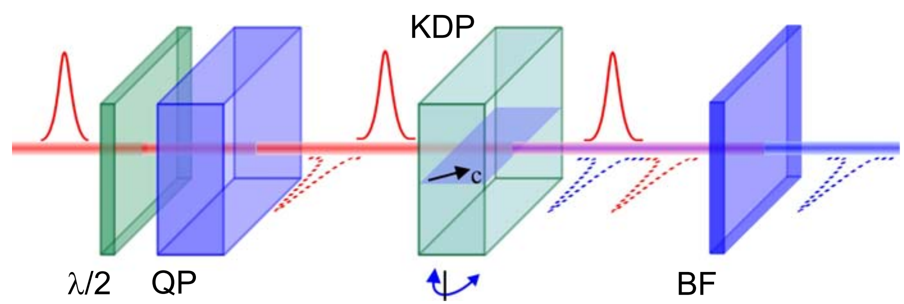

Type-II collinear SFG in KDP

Grice, U'Ren and IAW, Phys Rev. A., 64, 1 (2001)

Compact spectral shearing interferometer

Radunsky, Gorza, Wasylczyk and IAW, Opt. Lett., ***32*** *181 (2007*

- Simplified geometry for 20fs - 500 fs pulses

Another
Ridiculous
Acronym for
Interferometric
Geometrically-simplified
Noniterative
E-field
Extraction

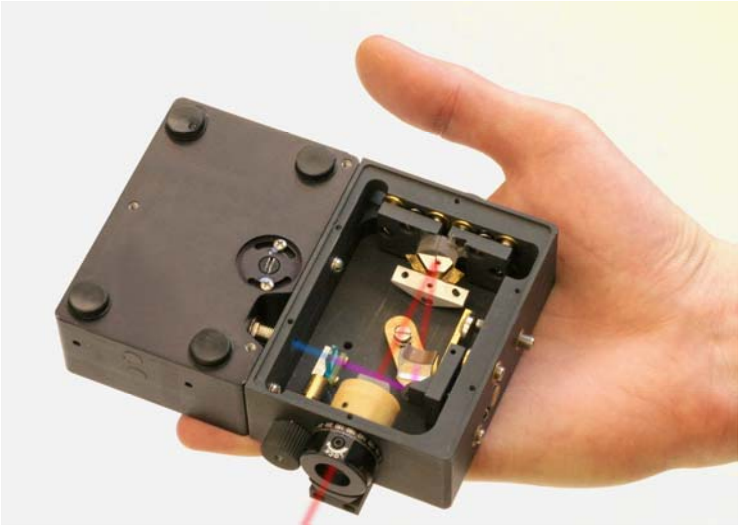

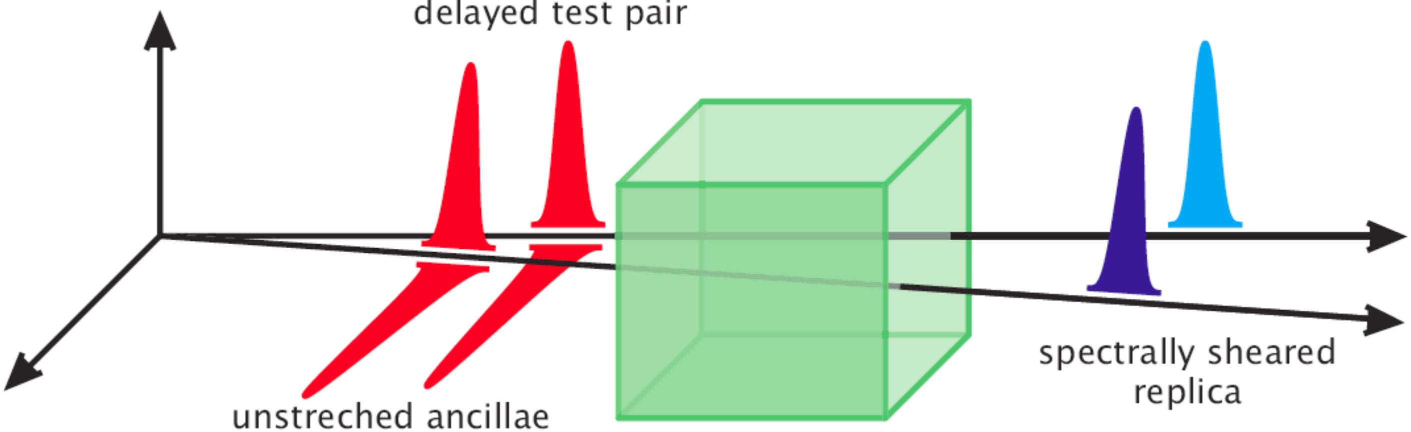

ARAIGNEE operation

Experimental Results: accuracy is verified by measuring the spectral phase after a known applied dispersion

Experiment vs. Theory

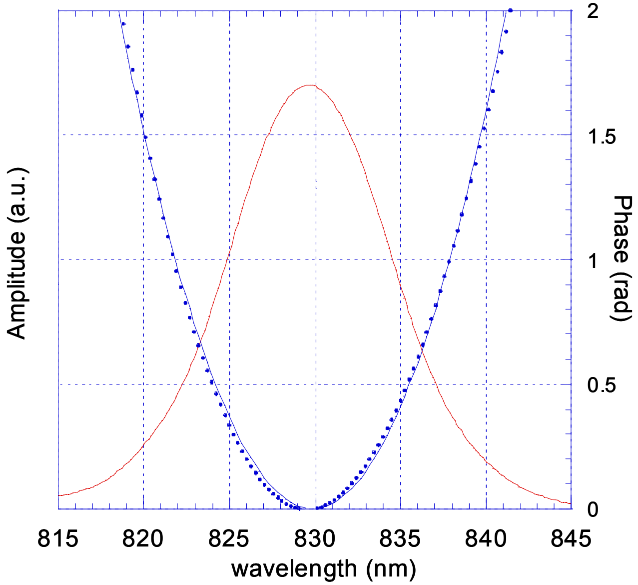

Measured GDD: **4160 fs²**

Theoretical value: **4175.5 fs²**

< 1% error

Mai-Tai pulse: 80fs, centered at 830nm;

Dispersion: BK7 glass, 10cm

LX-SPIDER vs. SPIDER

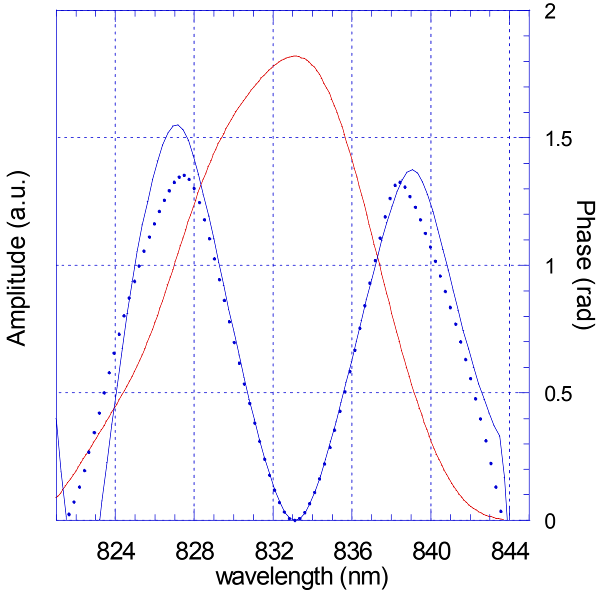

Shaped pulse from a CPA system

Linear spectral shearing interferometry

J. Bromage and C. Dorrer, LLE, U. Rochester

We have an EOSI design suitable for single-shot acquisition

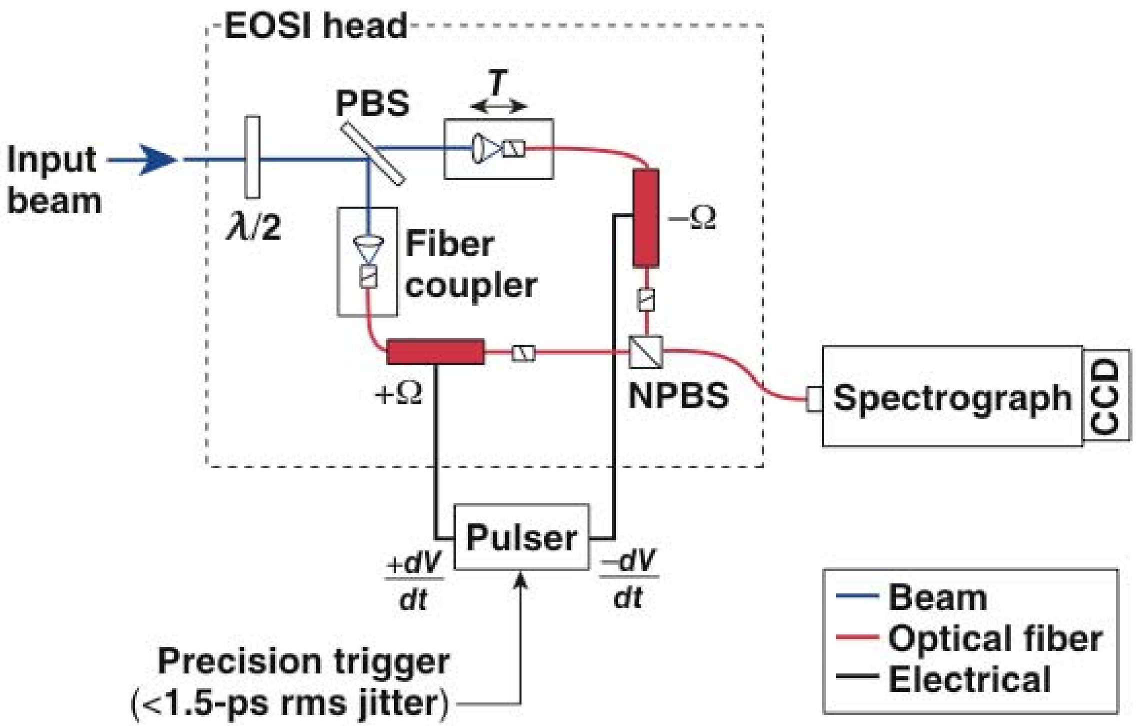

E14852

Linear spectral shearing interferometry

Measured second-order phase (ϕ_2) over wide range and good agreement with autocorrelation measurements

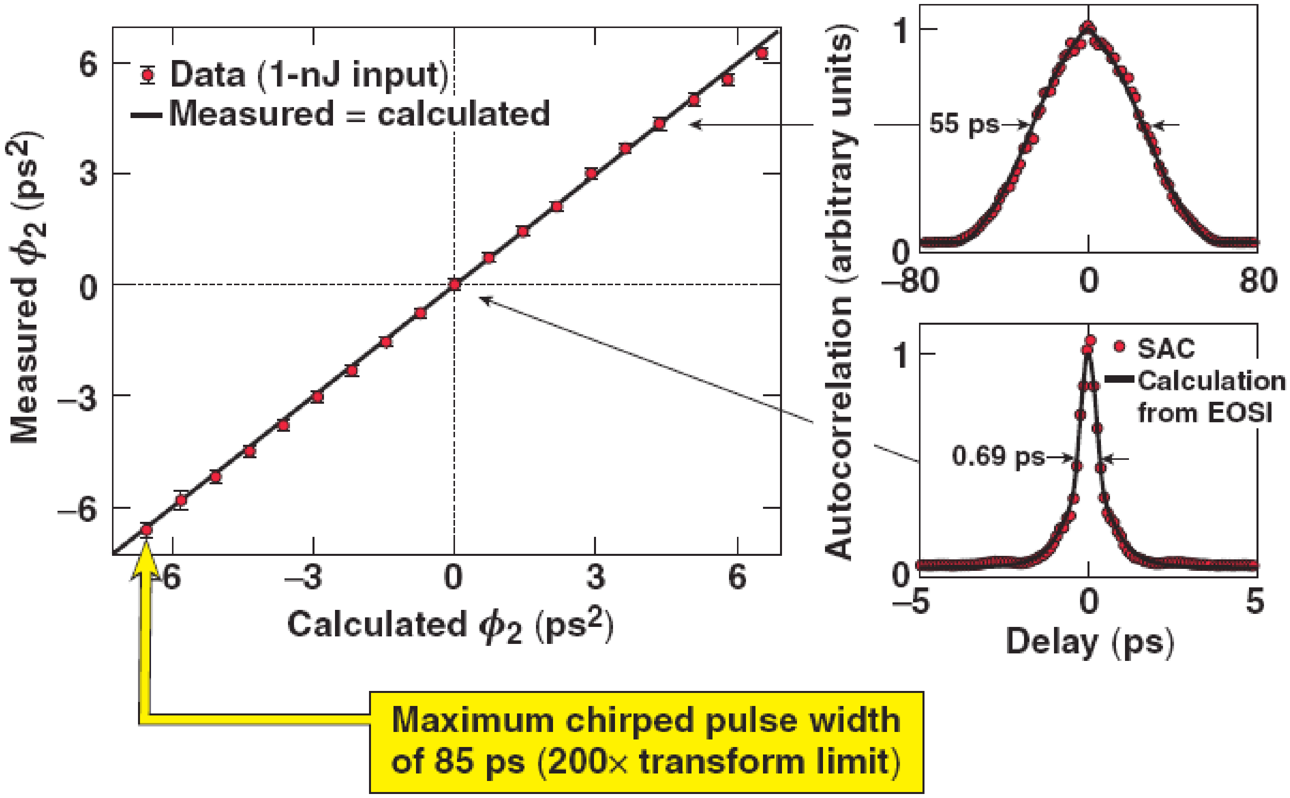

E14735

Outline

I . Introduction
II.General principles of pulse characterization
III. SPIDER
IV. Spatial coding
V. Long crystals
VI. Into the attosecond regime

A classic reinterpreted: the XUV autocorrelator

Nabekawa et al., Phys. Rev. Lett., ***97****, 153904 (2006)*

2-photon absorption generates molecular ions N_2^+

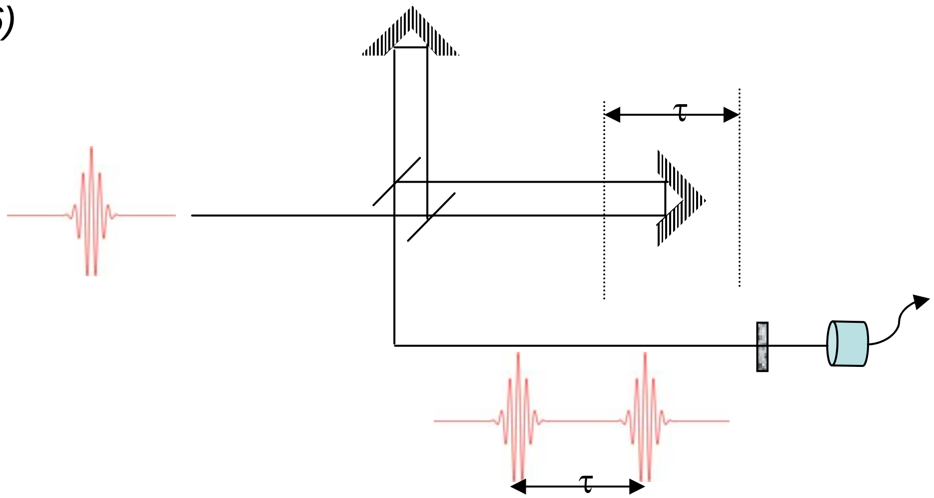

$$I(\tau) = \int_{-T}^{T} dt\, \left| E(t) + E(t+\tau) \right|^4$$

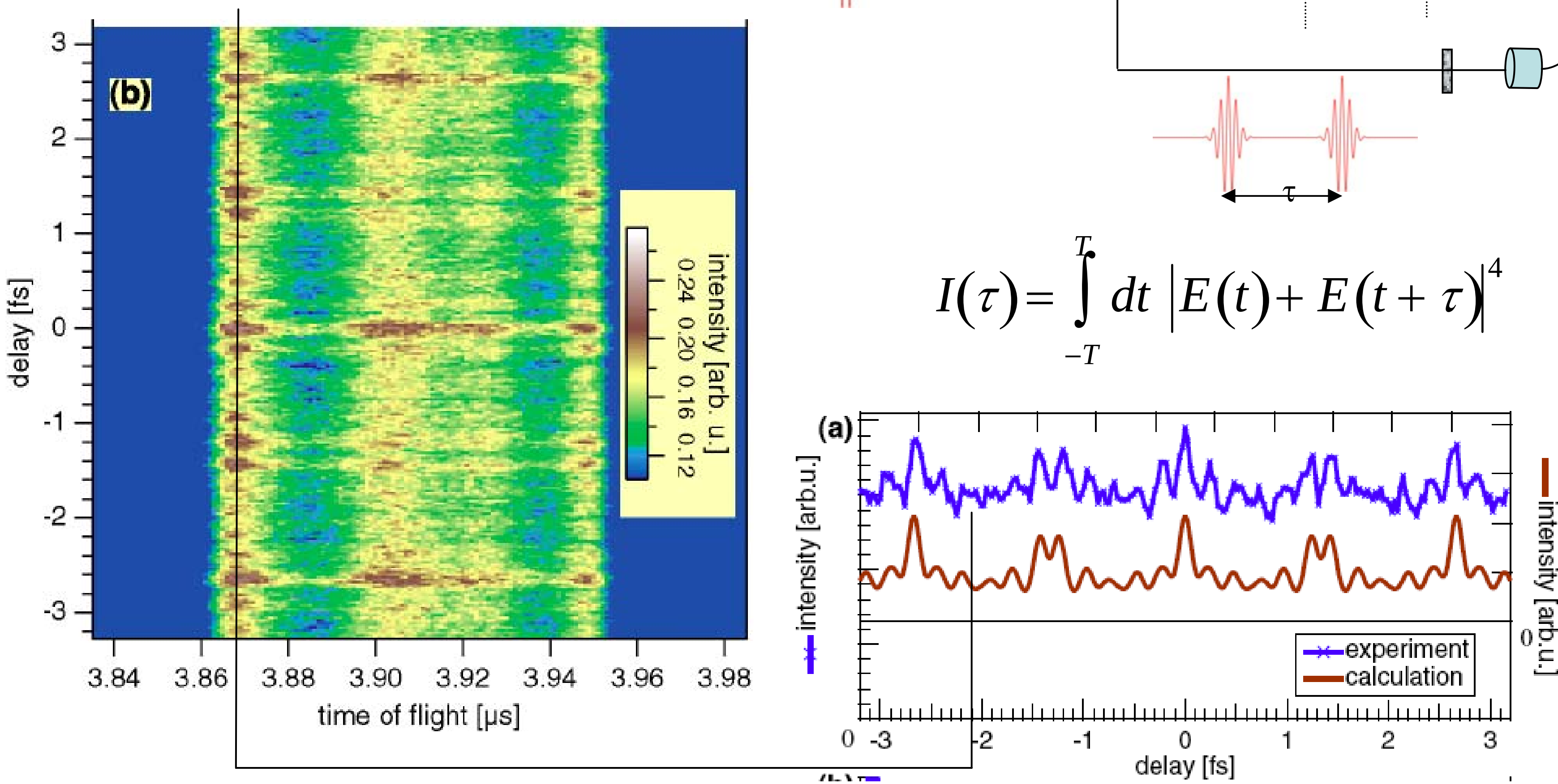

Require non-stationary filters with response times comparable to the pulse duration.

Temporal Phase modulation $N(t) = e^{i\Phi \cos \omega t}$

$E(t)$ $E_o(t) = e^{i\Omega t} E(t)$

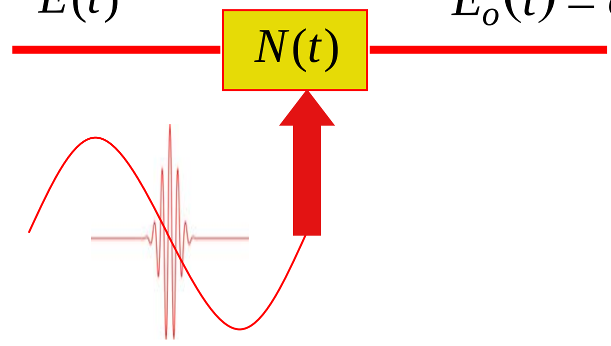

Linear phase modulation

Frequency shift

$E(t)$ $E_o(t) = e^{i\vartheta t^2} E(t)$

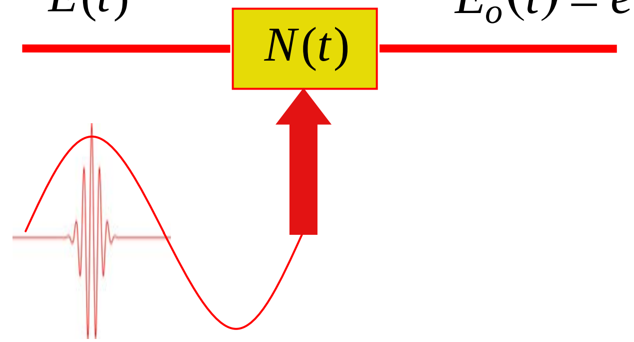

Quadratic phase modulation

Frequency chirp

Nonlinear optics in the XUV

Electron liberated by VUV pulse
is accelerated in the optical field

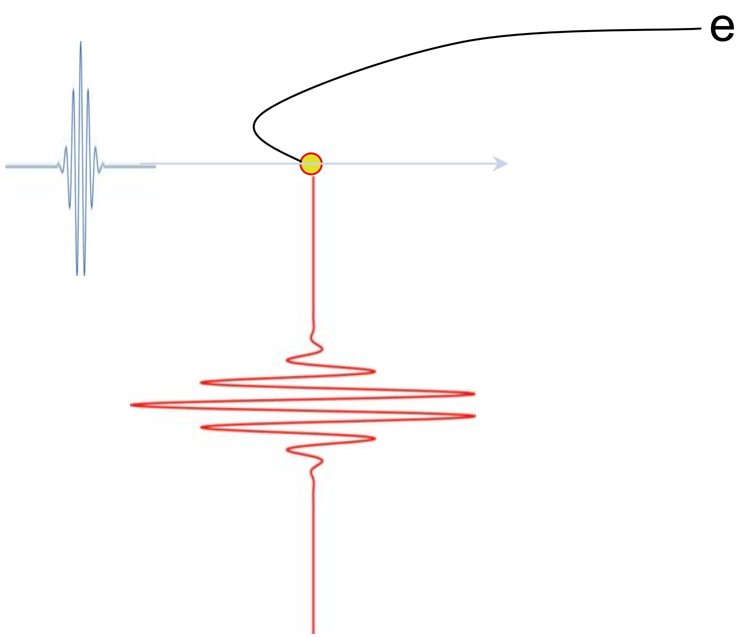

Electron energy

$$E = \vec{v}^{\,2}(t)$$

$$= v^2 + 2\vec{v}\cdot\vec{A}(t_o) + A^2(t_o)$$

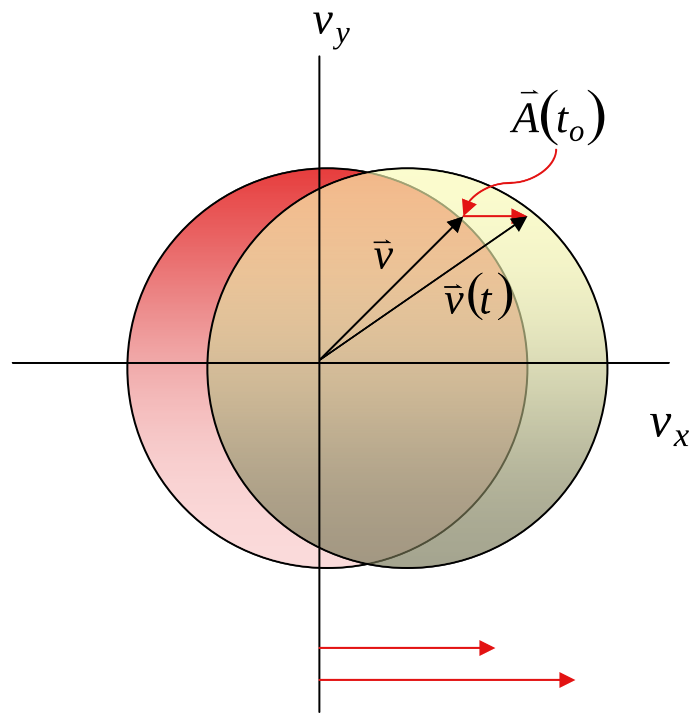

$$\vec{v}(t) = \vec{v} + \left(\vec{A}(t_o) - \vec{A}(t)\right)$$

Final Electron velocity

Electron Velocity at ionization

Optical vector potential at ionization

Photoelectron spectra

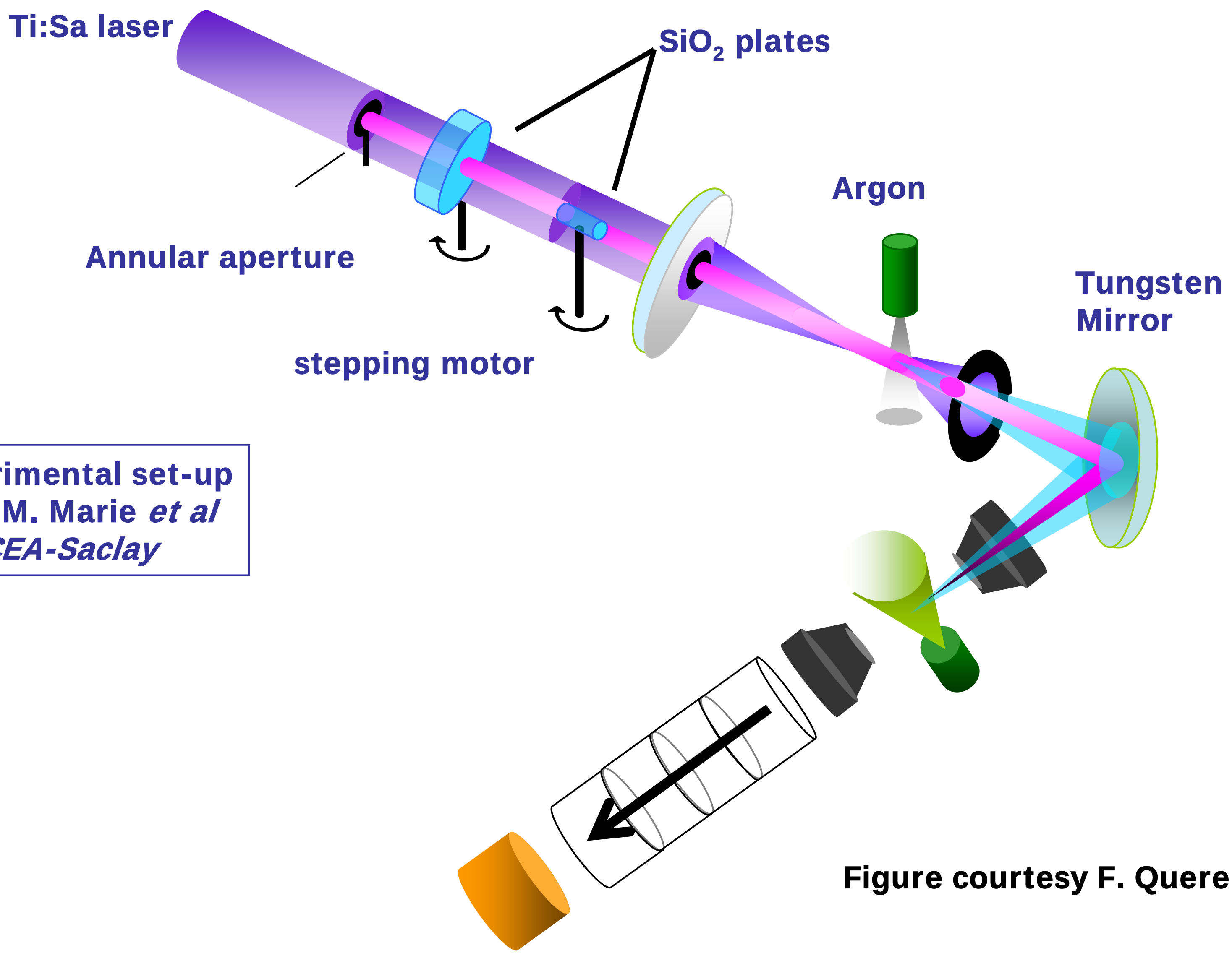

Experimental set-up
of P.M. Marie *et al*
CEA-Saclay

Figure courtesy F. Quere

Nonlinear optics in the XUV

Long XUV pulse regime:

Electron liberated by VUV pulse absorbs a photon from the optical field

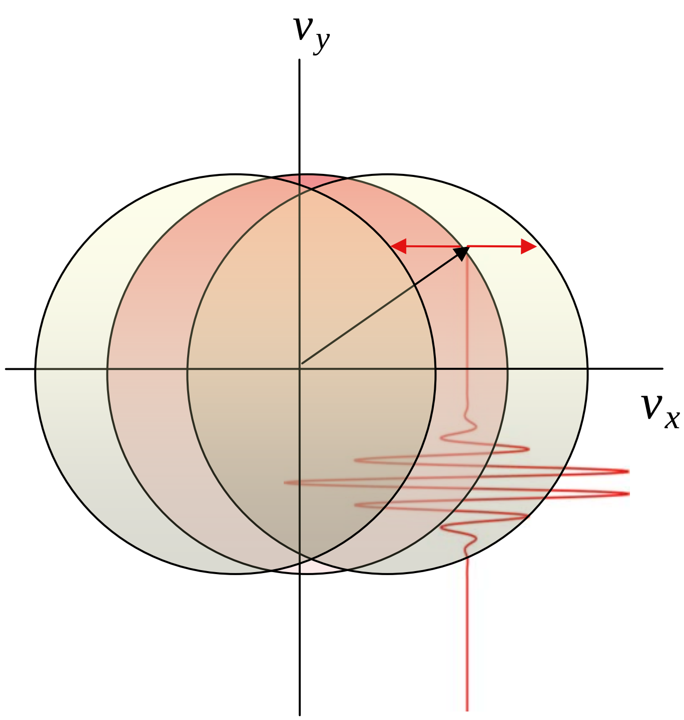

Electron energy

$$E = v^2 + U_p + n\omega_L$$

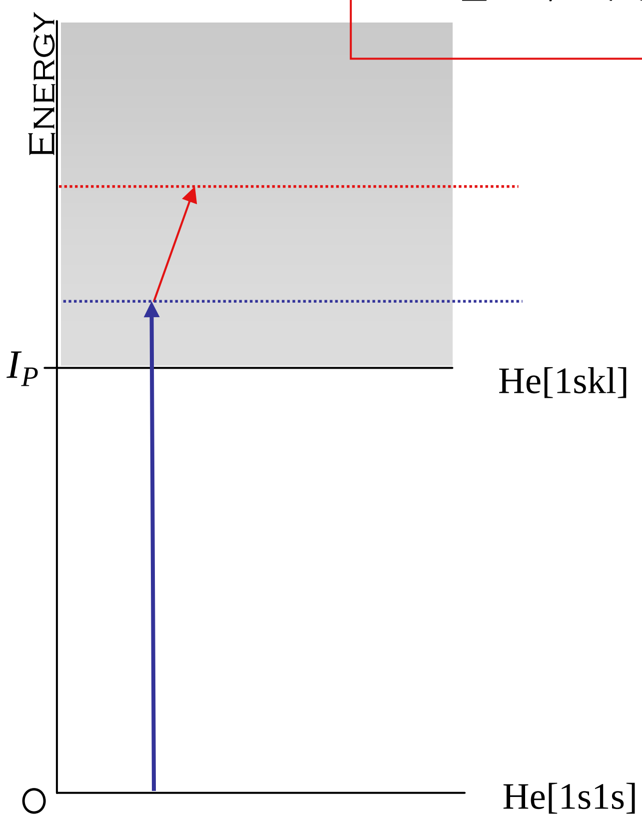

Attosecond measurements using PE sidebands

1-photon sidebands on an XUV pulse train

*Paul et al, Science, **292**, 1689 (2001)*

Interference of +/- orders yields phase difference

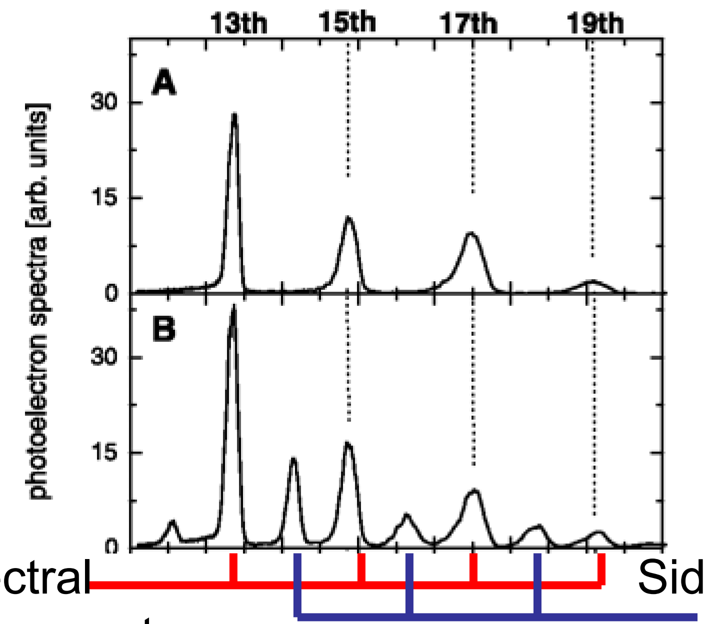

Spectral components of the pulse

Sidebands

(Pulse+IR pulse)

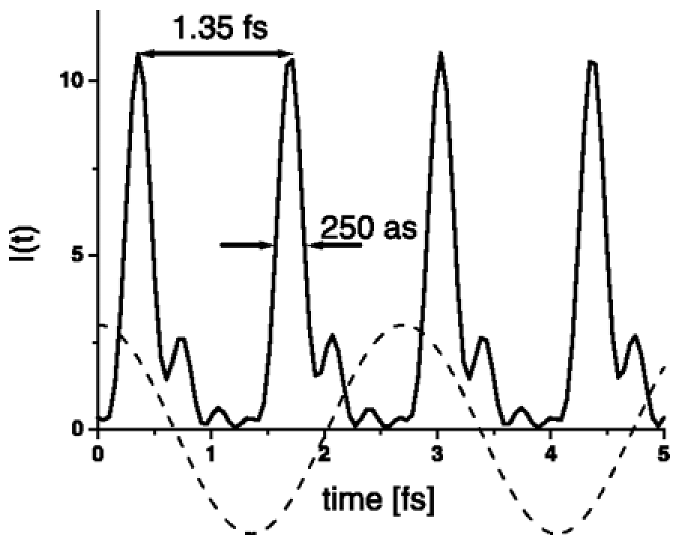

• Use as an energy-resolved cross-correlator: *Norin et al., Phys. Rev. Lett., **88**, 19301 (2002)*

XUV spectrography

Combines features of:

F. Quere et al, Topics in Applied Physics: Ultrafast Optics, Springer (2003)

Y. Mairesse and F. Quere, Phys. Rev. A, 71, 01140, (2005)

Spectral interferometry
Frequency-resolved gating

Scan delay between Ti:Sa and XUV

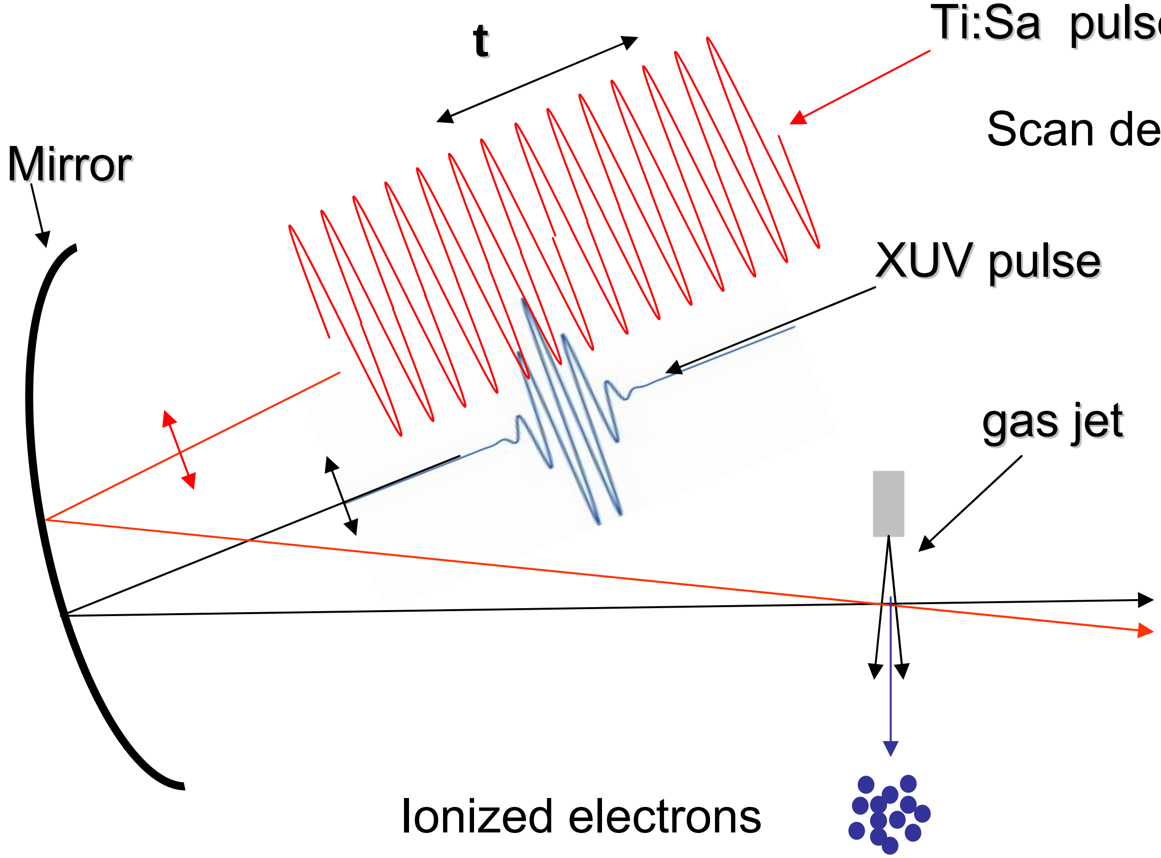

XUV spectrography: CRAB-FROG

Photoelectron spectra from Saclay; P. Salières *et al* *(Figure courtest P. Salieres and F. Quere)*

Spectrogram of a train of attosecond pulses

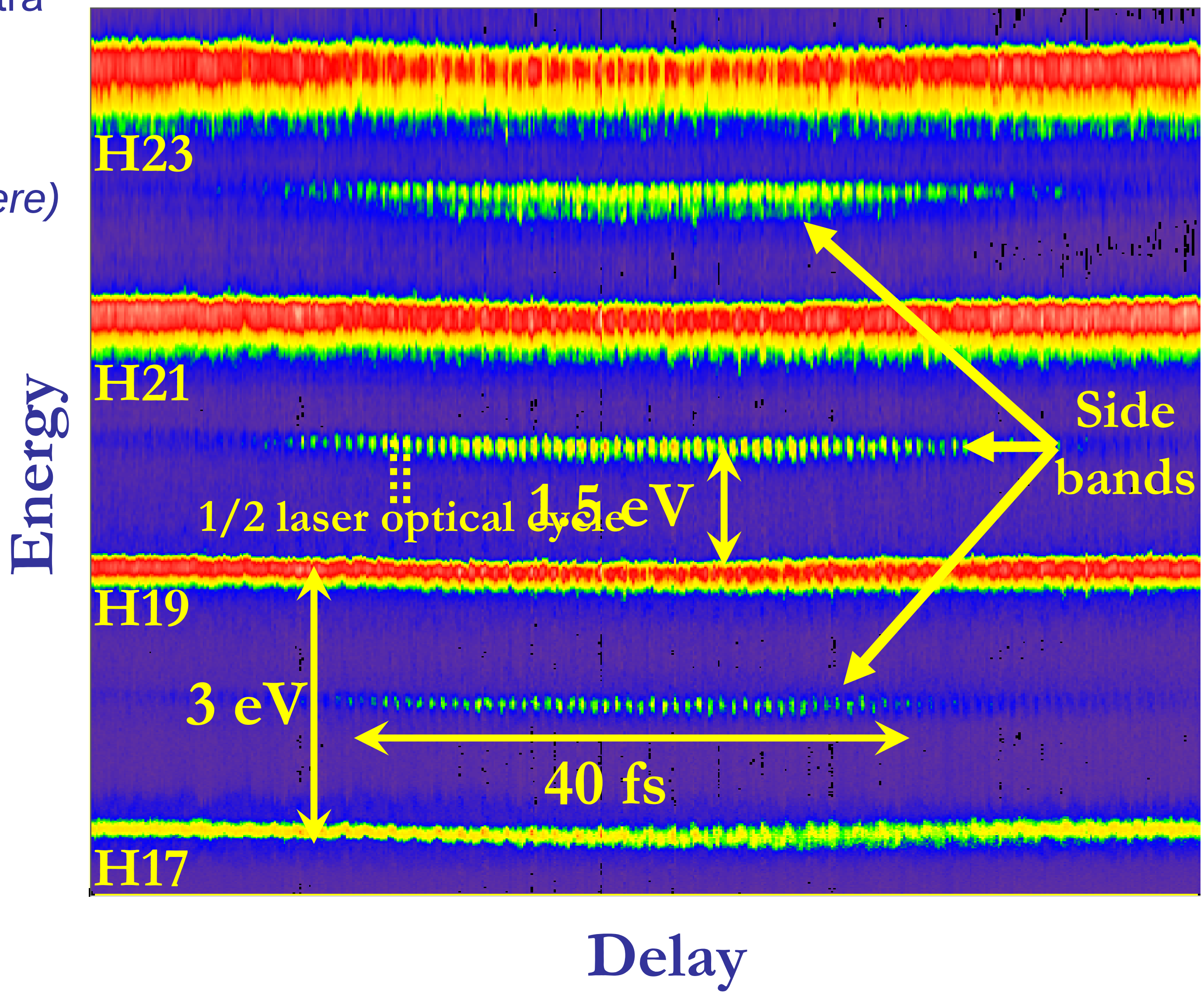

XUV spectrography: CRAB-FROG

Complete Reconstruction of Attosecond Bursts

Nonlinear spectrography using a phase-gate

Inversion using PCGP algorithm - retreives both XUV and IR pulse fields (Simulation)

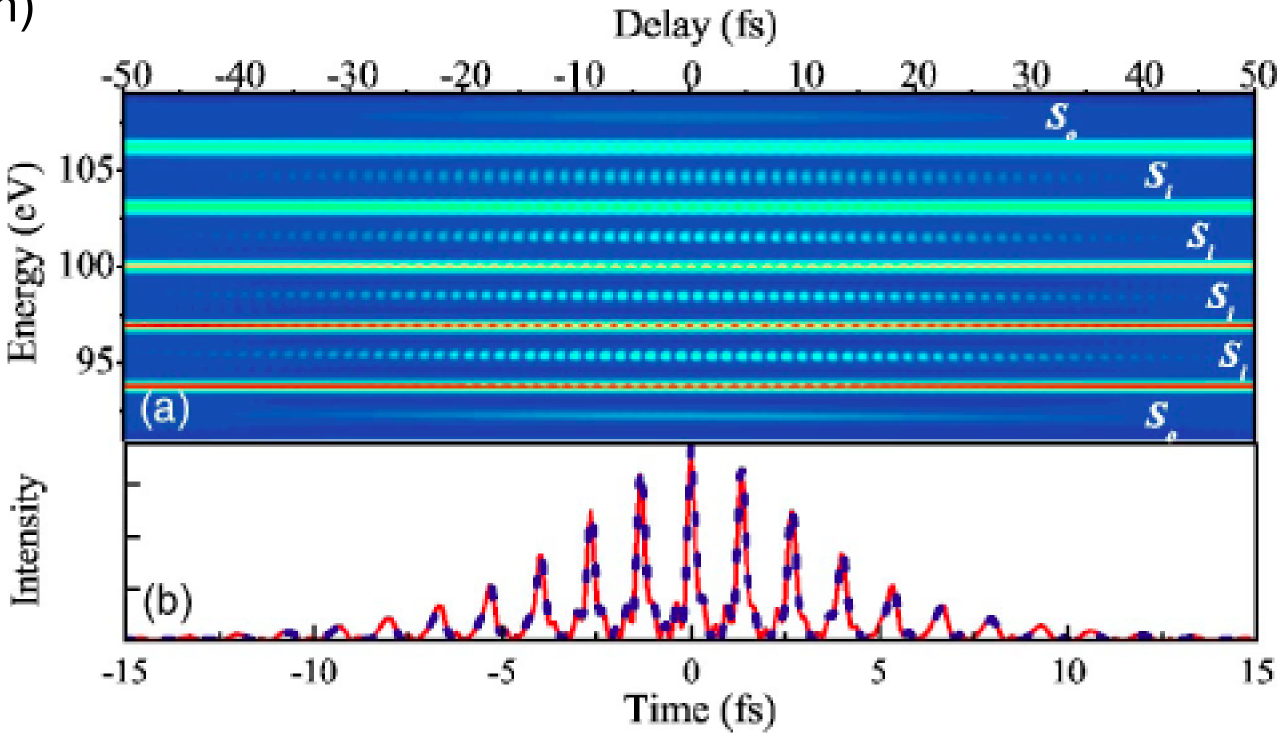

Y. Mairesse and F. Quere, Phys. Rev. A, 71, 01140, (2005)

XUV CRAB-FROG

- Simple to implement
- Works for large range of pulse durations
- Well-characterized reference needed
- Complicated iterative inversion

	Sideband w/harmonic	
Range	>0 as → >2 fs	
Experimental Parameter sensitivity	$\vec{A}(x,t)$ ω_L ~~E~~	

XUV chronocyclic tomography

E. Kosik et al, Topics in Applied Physics: Ultrafast Optics, Springer (2003)

E. Kosik, A. Wyatt, L. Corner, E. Cormier and I. A. Walmsley, Jnl. Mod. Opt., 52, 361, (2005)

Measure PE spectra for different phase-space rotations of electron
Time-frequency distribution

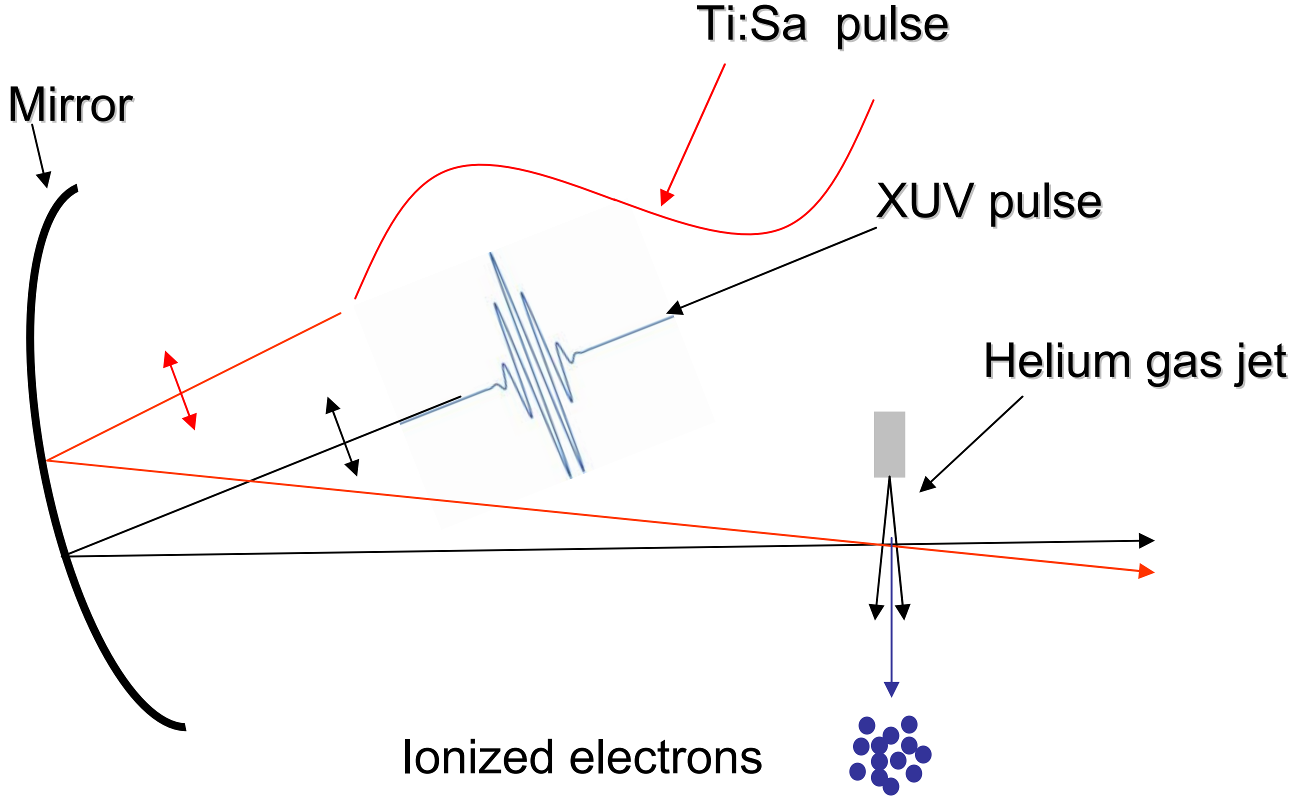

Photoelectron acceleration

Calculated photoelectron spectra as a function of delay between the optical and XUV pulses for various pulse durations

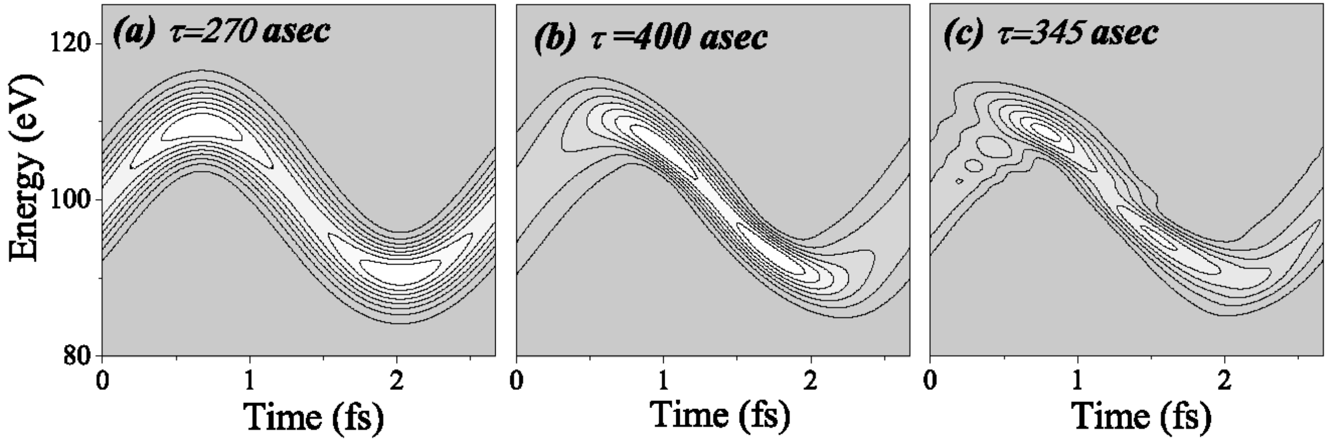

Figure courtesy F. Quere

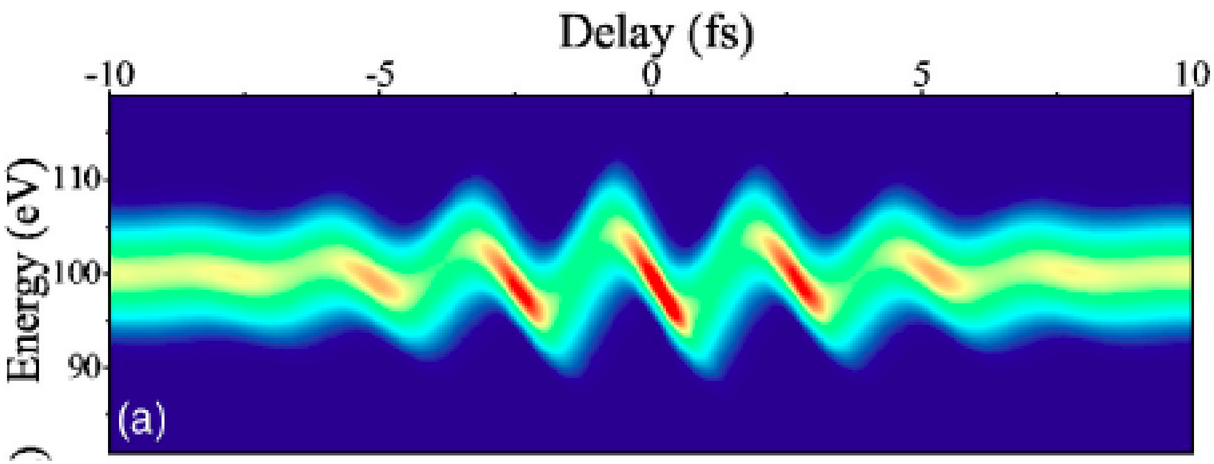

Y. Mairesse and F. Quere, Phys. Rev. A, 71, 01140, (2005)

XUV cross-correlator

Use isolated attosecond pulse to measure phase-stabilized optical pulse

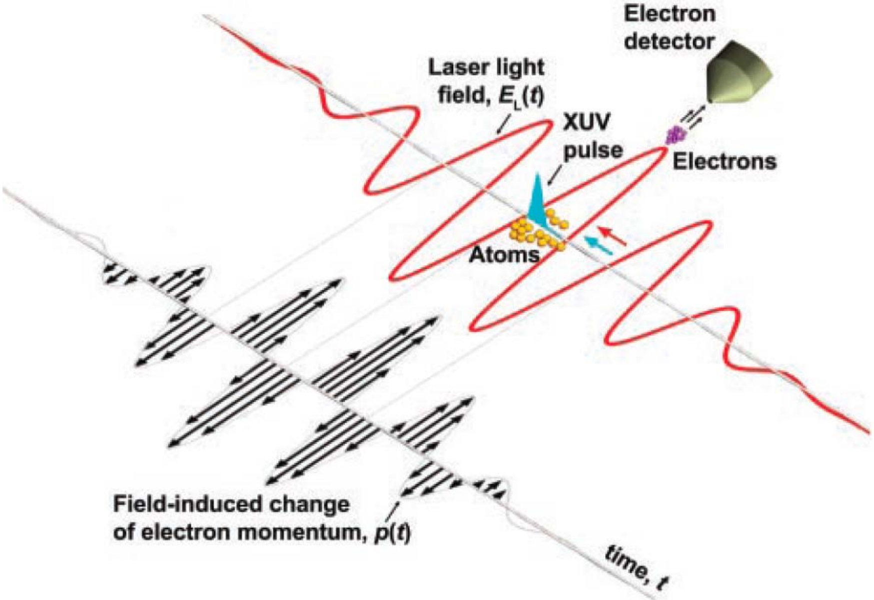

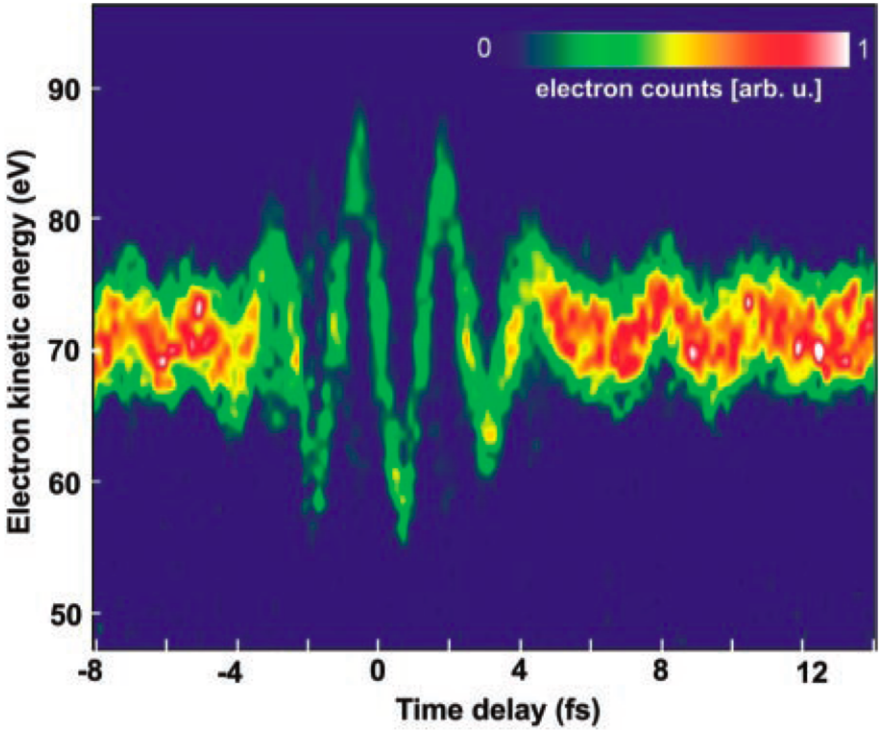

Goulielmakis et al, Science, 305, 1267, 2004

XUV chronocyclic tomography

Quadratic phase modulation and “streaking”

Phase modulation
“Rotates” spectrogram

More complicated distortions for longer pulses

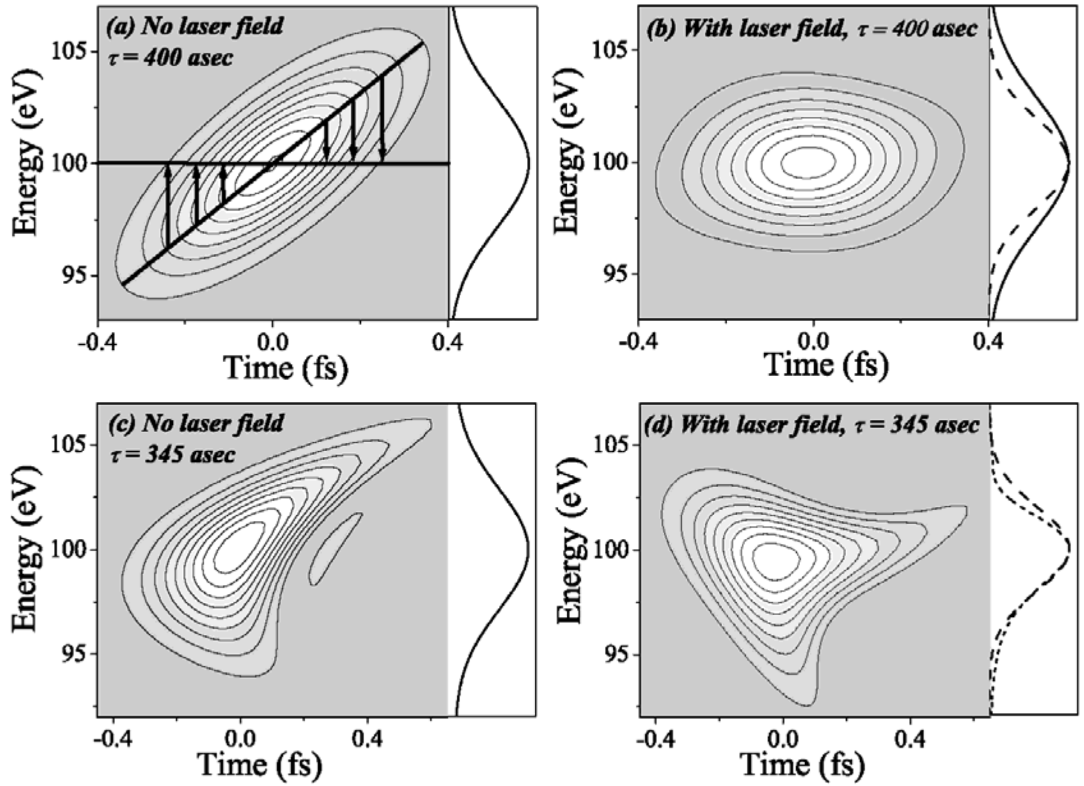

F. Quere et al, Topics in Applied Physics: Ultrafast Optics, Springer (2003)

XUV Chronocyclic tomography

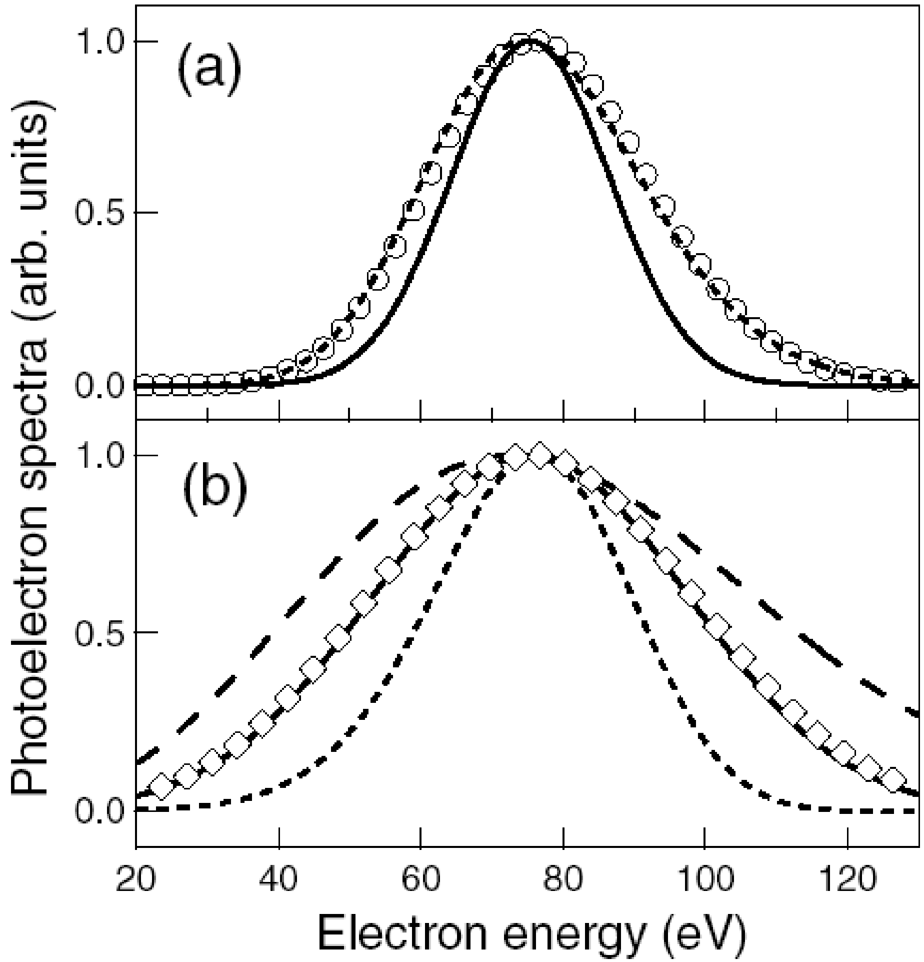

$$\vec{v}(t) = \vec{v} + \vec{A}_o \omega_L t^2$$

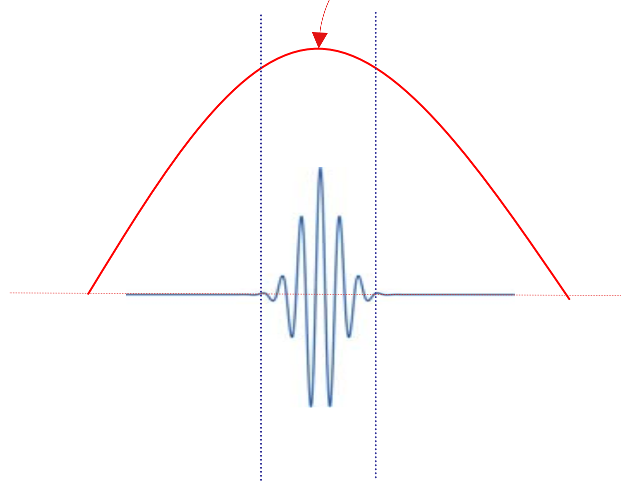

Quadratic change of field near peak of optical cycle provide the necessary chronocyclic phase space rotation.

<u>Atto-Time-to-frequency converter</u>

*J. Itatani et al, Phys. Rev. Lett., **88**, 173903 (2002)*

XUV Chronocyclic tomography

Principle of simplified tomography

*SCT: C. Dorrer and I. Kang, Opt. Lett., **90**, (2003)*

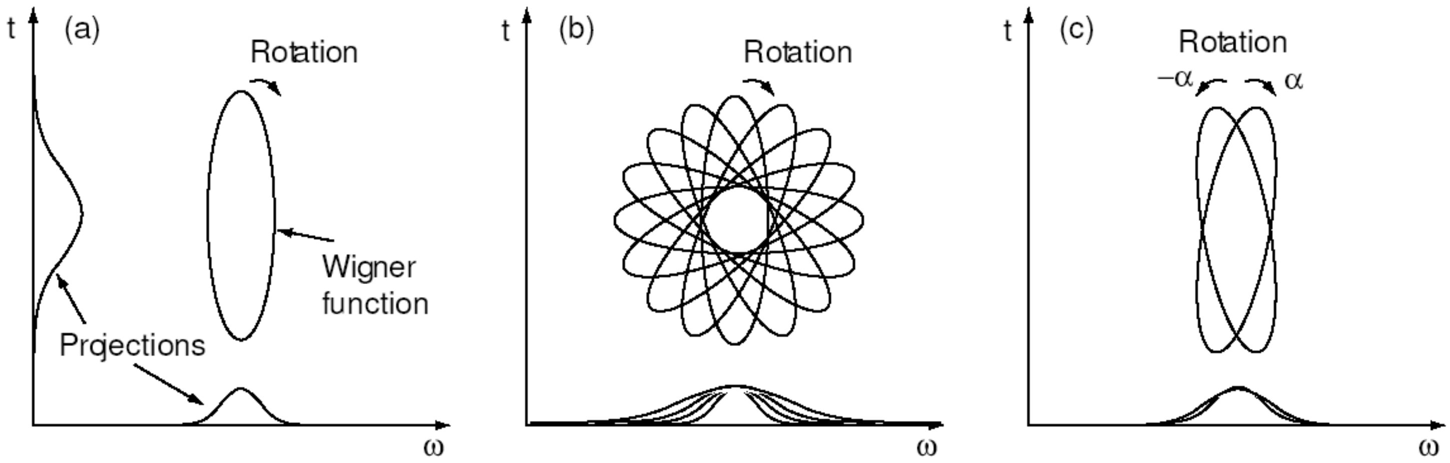

Pulse reconstruction from two photoelectron spectra

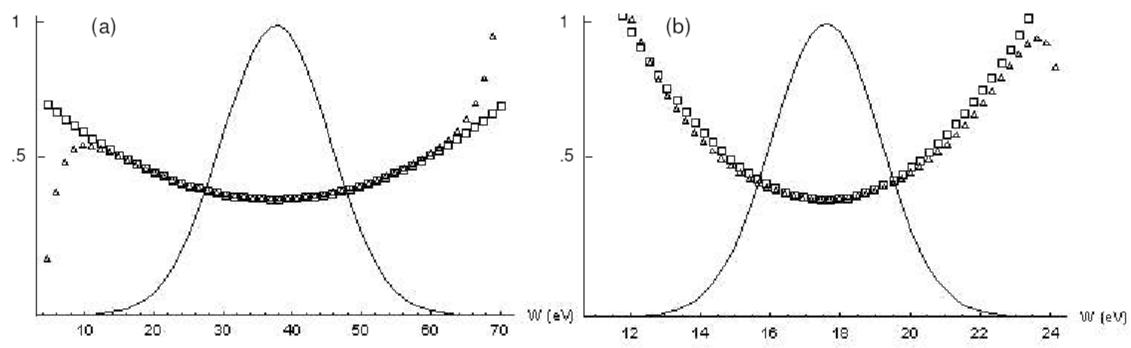

XUV SCT: E. Kosik et al, Topics in Applied Physics: Ultrafast Optics, Springer (2003)

I . Introduction
II.General principles of pulse characterization
III. XUV metrology using photoelectrons
III. Direct XUV metrology

Direct XUV measurement

Complete pulse characterization directly in the XUV

*Cormier et al, PRL, **94,** 033905 (2005)*
*Mairesse et al PRL, **94,** 173903 (2005)*

- Better signal to noise
- Realistic single (few) shot operation

Generate spectrally-sheared HHG using spectrally sheared drive pulses

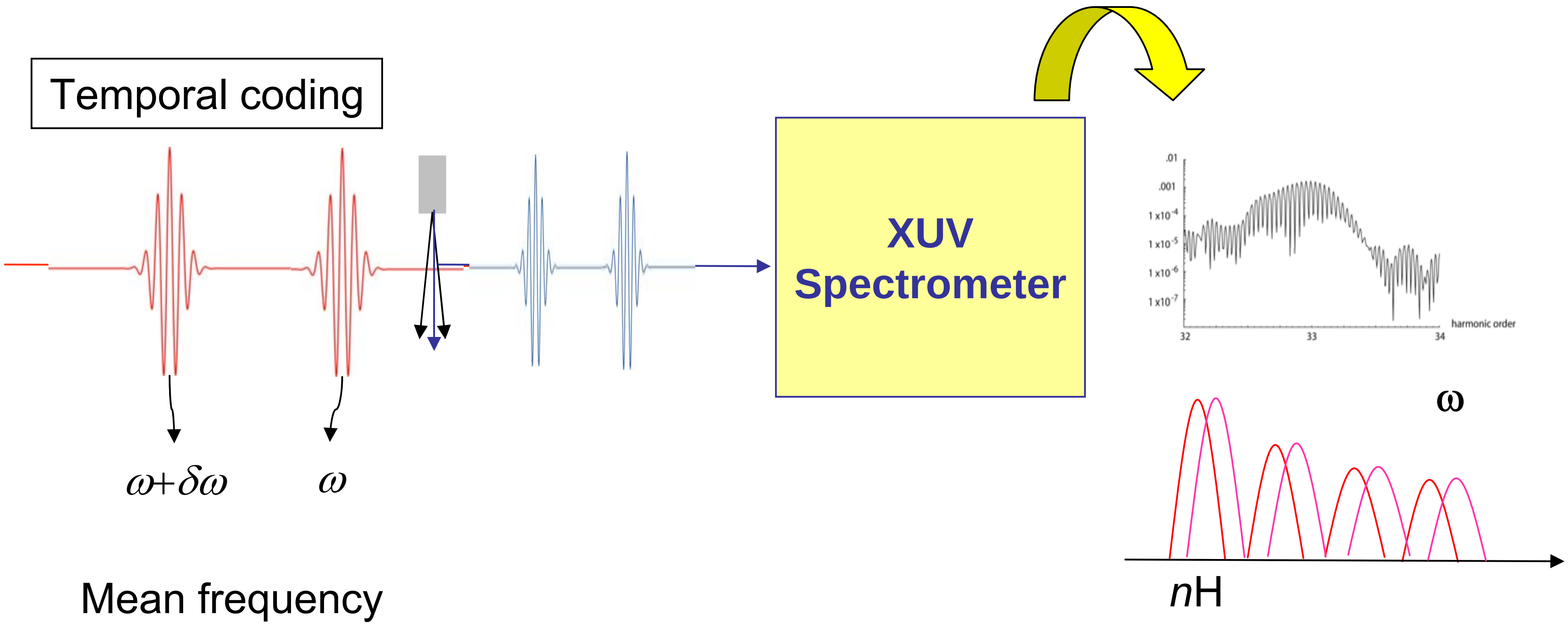

Direct XUV measurement

Experimental implementation: *Mairesse et al PRL 94 173903 (2005)*

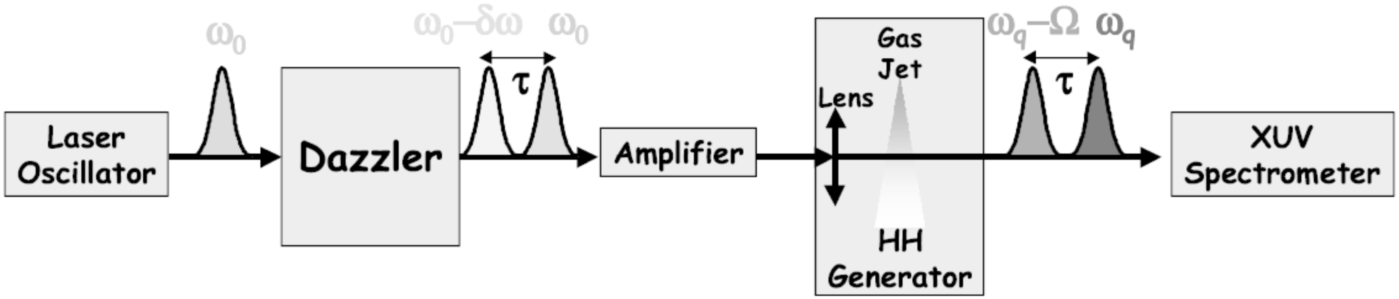

Experimental data for single harmonic:

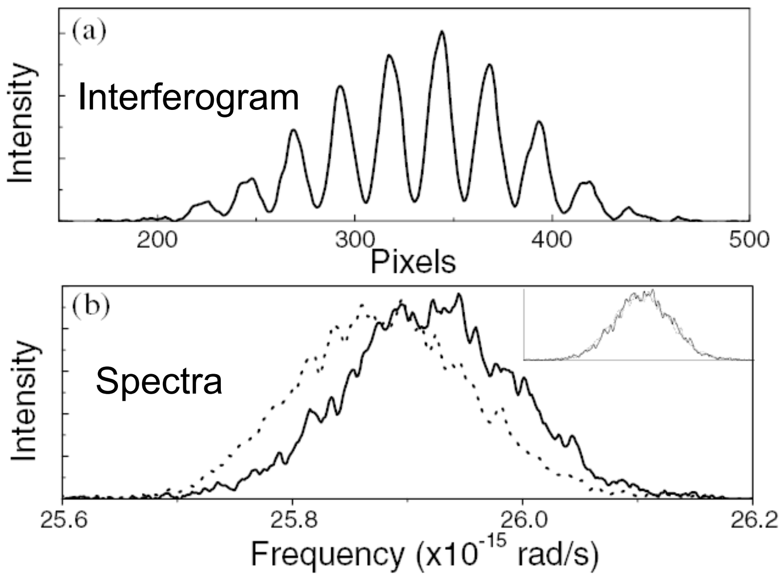

Reconstructed pulse amplitude and phase

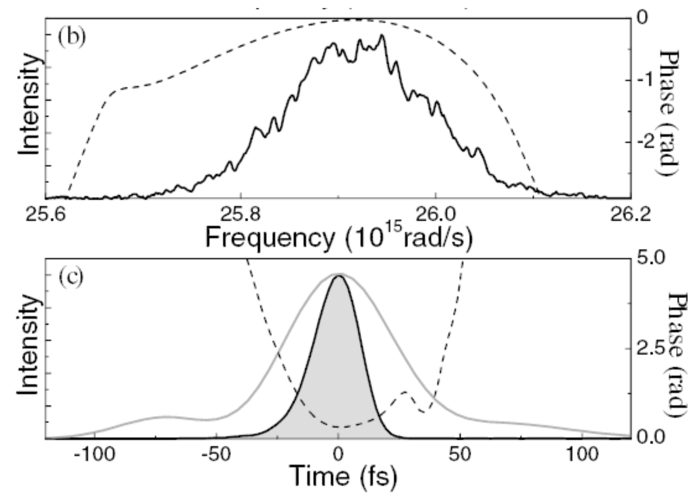

Direct XUV measurement

Numerical simulations of XUV-SPIDER operation: *Cormier et al, PRL 94 033905 (2005)*

HHG spectrum

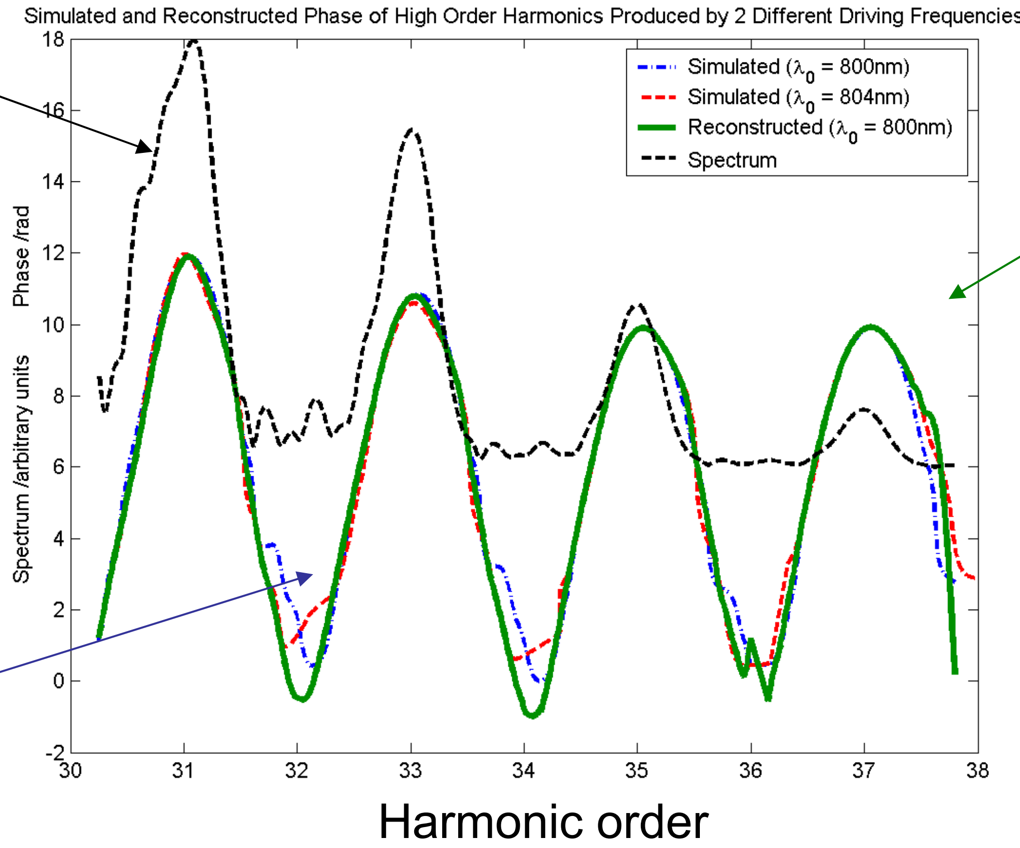

Reconstructed pha

800 nm phase (simulation)

804 nm phase (simulation)

Spectral shear scaling depends on drive frequency

Direct XUV measurement

Spatial coding of spectral interference

Reduced spectral resolution: operates at the sampling limit for the test pulse

Avoids pulse energy limit for sequential pulses

Enables extraction of space-time coupling even without spectrally-sheared driving pulses

Spatial coding

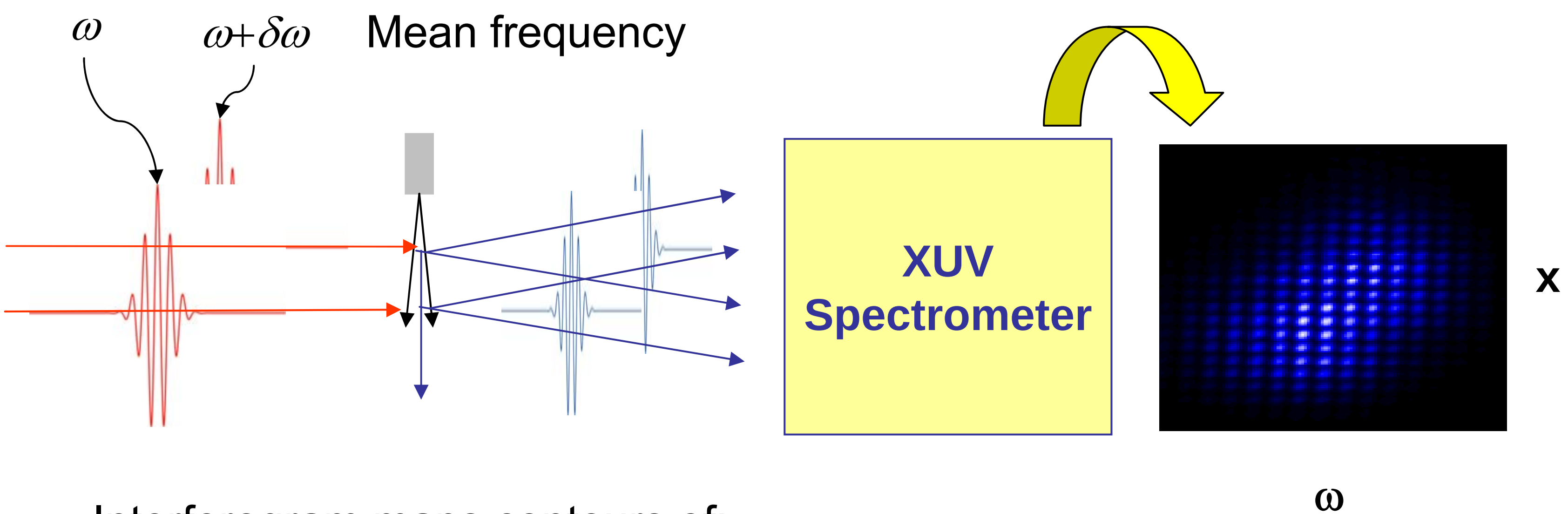

Interferogram maps contours of:

$$\phi(\omega-\omega_0,x)-\phi(\omega-\omega_0+\Omega,x+\Delta)+Kx+\omega\tau$$

Direct XUV measurement

Experimental arrangement:

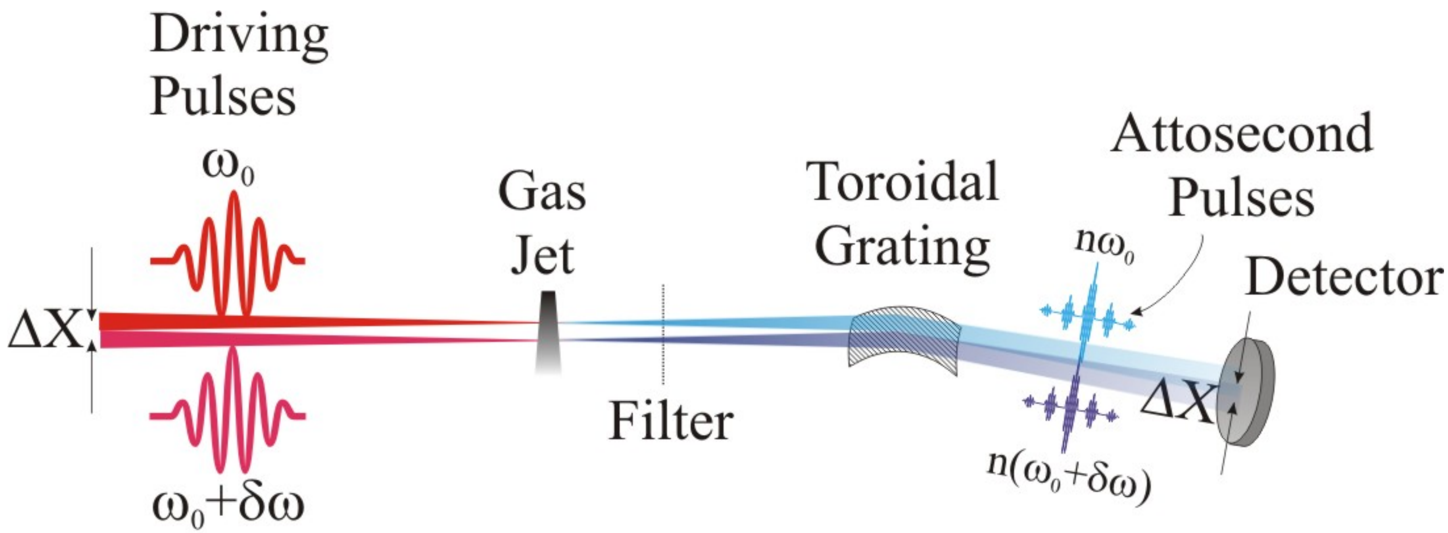

<7fs pulses from HCF compressor and Michelson interferometer

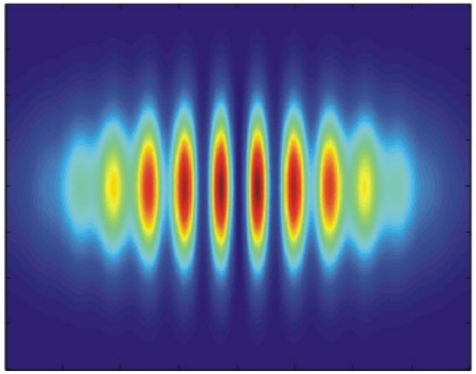

With no spectral shear on the drive pulses, the interferogram maps contours of:

$$\phi(\omega-\omega_0,x)-\phi(\omega-\omega_0,x+\Delta)+\omega\tau$$

Conclusions

I . Introduction
II.General principles of pulse characterization
III. SPIDER
IV. Spatial coding
V. Long crystals
VI. Into the attosecond regime

VII. Applications